

# Design and evaluation of BOOGIE: a collector for the analysis of cloud composition and processes

Mickael Vaitilingom<sup>1,2\*</sup>, Christophe Bernard<sup>3</sup>, Mickaël Ribeiro<sup>1</sup>, [Christophe Verhaege<sup>1,4</sup>](#), [Christophe Gourbeyre<sup>1</sup>](#), Christophe Berthod<sup>5</sup>, Angelica Bianco<sup>1</sup>, Laurent Deguillaume<sup>1,3\*</sup>

<sup>1</sup> Laboratoire de Météorologie Physique, UMR 6016, CNRS, Université Clermont Auvergne, 63178 Aubière, France.

<sup>2</sup> Laboratoire de Recherche en Géosciences et Énergies, EA 4539, Université des Antilles, 97110 Pointe-à-Pitre, France.

<sup>3</sup> Observatoire de Physique du Globe de Clermont-Ferrand, UAR 833, CNRS, Université Clermont Auvergne, 63178 Aubière, France.

<sup>4</sup> Institut Universitaire de Technologie Clermont Auvergne - site de Montluçon, Université Clermont Auvergne, 03100 Montluçon, France.

<sup>5</sup> Division Technique de l'Institut National des Sciences de l'Univers, UAR 855, CNRS, 91190 Gif-sur-Yvette, France.

Correspondence to: Laurent Deguillaume (laurent.deguillaume@uca.fr) and Mickael Vaitilingom (mickael.vaitilingom@univ-antilles.fr)

**Abstract.** In situ cloud studies are fundamental to study the variability in cloud chemical and biological composition as a function of environmental conditions and assess their potential for transforming chemical compounds. To achieve this objective, cloud water collectors have been developed in recent decades to recover water from clouds and fogs using different designs and collection methods. In this study, a new active ground-based cloud collector was developed and tested for sampling cloud water to assess the cloud microbiology and chemistry. This new instrument, BOOGIE, is a mobile sampler for cloud water collection *easy to operate* with the objective of being cleanable and sterilisable, respecting chemical and microbial cloud integrity, and presenting an efficient collection rate of cloud water. Computational fluid dynamics simulations were performed to theoretically assess the capture of cloud droplets by this new sampler. A 50% collection efficiency cutoff of 12  $\mu\text{m}$  has been estimated. The collector was deployed at Puy de Dôme station under cloudy conditions for evaluation. The water collection rates were measured at  $100 \pm 53 \text{ mL h}^{-1}$  for a collection of 21 cloud events; considering the measured liquid water content, the sampling efficiency of this new collector has been estimated at  $69.7 \pm 11\%$  over the same set of cloud events. BOOGIE was compared with other active cloud collectors commonly used by the scientific community (Cloud Water Sampler and Caltech Active Strand Cloud Collector version 2). The three samplers presented similar collection efficiencies (between 53% and 70% on average). The sampling process can affect the endogenous cloud water microflora, but the ATP/ADP ratio obtained from the samplers indicate that they are not stressful for the cloud microorganisms. The chemical composition of hydrogen peroxide, formaldehyde and major ions are similar between the collectors; a significant variability is observed for magnesium and potassium that are the less concentrate ions. The differences between collectors are the consequence of different designs, and the intrinsic homogeneity in the chemical composition within the cloud system.

**Keywords:** Cloud chemistry, monitoring, cloud water collector, chemical composition, biological composition.

**a supprimé :** Biological, Organics, Oxidants, soluble Gases, inorganic Ions and metal Elements

**Commenté [LD1]:** Two persons were added to the co-authors. They have been involved in the experimental evaluation of the air flow inside the BOOGIE collector. They participated to the corrections of the submitted manuscript.

**a supprimé:** Cloud/fog droplets comprise a myriad of chemical compounds and are living environments in which microorganisms are present and active. These chemical and biological elements can evolve in various ways within the cloud system, and the aqueous transformation of chemicals contributes to atmospheric chemistry.

**a supprimé:** Few turbulences have been observed inside the collector and a

## 54 1 Introduction

55 The chemical composition of clouds is highly complex because it results from various processes: (1) the mass  
56 transfer of soluble compounds from the gas phase into cloud droplets, (2) dissolution of the cloud condensation  
57 nuclei released into the aqueous phase as a complex mixture of soluble molecules, and (3) photochemical and  
58 biological transformations leading to new chemical products (Herrmann et al., 2015).

59 Field experiments to characterise this multiphasic medium were developed in the 1950s but increased in the 1980s  
60 because of precipitation acidification through sulphur oxidation in cloud droplets (Munger et al., 1983; Hoffmann,  
61 1986; Kagawa et al., 2021). These studies have highlighted that cloud and fog processing is efficient and plays a  
62 major role in air pollution by transforming gases and aerosol particles. Numerous investigations have focused on  
63 inorganic compounds that control aqueous-phase acidity (Pye et al., 2020). The production of strong acids has  
64 been assessed because it increases particle mass when clouds/fogs evaporate and leads to acidic deposition when  
65 clouds precipitate (Tilgner et al., 2021). Early in the 1990s and much more so in the 2000s, researchers investigated  
66 the composition of dissolved organic matter in cloud/fog water which has multiple natural and anthropogenic  
67 sources of primary or secondary origins (Herckes et al., 2013). Based on scientific issues, specific classes of  
68 compounds have been targeted, such as short-chain carboxylic acids and carbonyls (Löflund et al., 2002; Munger  
69 et al., 1995; Sun et al., 2016) and more recently carbohydrates and amino acids (Triesch et al., 2021; Renard et al.,  
70 2022). Attention has also been paid to the detection of pollutants with strong sanitary effects, such as [polycyclic](#)  
71 [aromatic hydrocarbon \(PAH\)](#), phenols, and phthalates (Lüttke et al., 1999; Li et al., 2010; Lebedev et al., 2018;  
72 Ehrenhauser et al., 2012) because they can impact ecosystems through precipitation (Wright et al., 2018). Recent  
73 investigations using high-resolution mass spectrometry have revealed the complexity of the organic matrix, with  
74 thousands of detected molecules (Zhao et al., 2013; Cook et al., 2017; Bianco et al., 2018; Sun et al., 2021). This  
75 organic matter is processed during the cloud lifetime and has raised new scientific questions such as the formation  
76 of secondary organic aerosol by aqueous phase reactivity (“aqSOA”) (Blando and Turpin, 2000; Lamkaddam et  
77 al., 2021) and light absorbing material referring to brown carbon (“BrC”) (Laskin et al., 2015). Microorganisms  
78 are also present and active in cloud droplets (Amato et al., 2005; Vařtilingom et al., 2012; Xu et al., 2017; Hu et  
79 al., 2018). They can be incorporated because they serve as cloud condensation nuclei (Bauer et al., 2002;  
80 Deguillaume et al., 2008) and can impact cloud water composition through their metabolism by consuming or  
81 producing new molecules (Liu et al., 2023; Vařtilingom et al., 2013; Pailler et al., 2023). Many investigations have  
82 focused on biological cloud characterisation (Amato et al., 2017; Wei et al., 2017).

83 Monitoring cloud chemical and biological compositions is crucial for evaluating the role of key environmental  
84 parameters such as emission sources, atmospheric transport and transformations, and physicochemical cloud  
85 properties such as cloud acidity or microphysical cloud properties (liquid water content [LWC] and size  
86 distribution of cloud droplets). Specific sites or aircraft campaigns allow the collection of cloud water influenced  
87 by marine (Macdonald et al., 2018; Gioda et al., 2011), continental (Van pinxteren et al., 2016; Hutchings et al.,  
88 2009; Lawrence et al., 2023; Van Pinxteren et al., 2014) and urban emissions (Li et al., 2020; Guo et al., 2012;  
89 Herckes et al., 2002) over various continents (mainly Europe, North America, Asia). Owing to their poor  
90 accessibility and remoteness, certain geographical locations have been less investigated, such as the Arctic region  
91 (Adachi et al., 2022), tropical environments (Dominutti et al., 2022), or marine surfaces (Van Pinxteren et al.,  
92 2020). Field experiments combining cloud water and gaseous phase chemical characterisation have also been

93 conducted to evaluate the partitioning of molecules between these two phases and whether bulk cloud water obeys  
94 Henry's law (Van Pinxteren et al., 2005; Wang et al., 2020). Bulk aqueous cloud media are used for laboratory  
95 investigations to study the aqueous transformations induced by light and the presence of microorganisms  
96 (Schurman et al., 2018; Bianco et al., 2019).

97 Therefore, the scientific community requires regular and long-term measurements of cloud chemical and biological  
98 parameters. However, cloud sampling procedures are challenging. In recent decades, different samplers have been  
99 developed and deployed in the field, which can be operated under specific environmental conditions and present  
100 different collection efficiencies possibly impacted by meteorological conditions. These are commonly based on  
101 the impact of cloud droplets on the collector surface and avoid the collection of small droplets (<5 µm in diameter).  
102 Their collection efficiency and 50% collection cutoff diameter (d50) were calculated and estimated to evaluate the  
103 accuracy of droplet collection by the sampler. Monitoring of the microphysical cloud properties (LWC and size  
104 distribution) is required to assess this. These samplers refer to "bulk" cloud water collectors because they group  
105 droplets of different sizes. Many types of collectors can be listed: active or passive ground- or aircraft-based, and  
106 single- or multi-stage. Passive collectors are dependent on wind speed because the air needs to flow through them,  
107 allowing sampling. Active collectors are ground-based collectors through which air-containing droplets are forced  
108 to flow inside the system by devices such as pumps or ventilator fans. They have been designed and commonly  
109 used to obtain higher volumes of water required for laboratory investigations. Ground-based samplers are easy to  
110 install, inexpensive, and suitable for long-term observations. Samplers installed on aircrafts are less widely used,  
111 and recent developments by Crosbie et al. presenting a new axial cyclone cloud water collector have shown to  
112 strongly improve the collection efficiency of cloud droplets compared to previous samplers (Crosbie et al., 2018).  
113 All these samplers are described in reviews where their designs, their advantages, limitations are presented (Roman  
114 et al., 2013; Skarżyńska et al., 2006).

115 Two types of ground-based active samplers are often used by the scientific community to monitor cloud chemistry  
116 and microbiology: the Cloud Water Sampler (CWS) from Vienna University (Kruisz et al., 1993) and the Caltech  
117 Active Strand Cloudwater Collector (CASCC) from [California Institute of Technology](#) (Daube et al., 1987; Demoz  
118 et al., 1996; Collett Jr et al., 1990). These collectors have been adapted for long-term monitoring (Gioda et al.,  
119 2013; Guo et al., 2012; Deguillaume et al., 2014; Renard et al., 2020) and specific field campaigns (Wieprecht  
120 et al., 2005; Van pinxteren et al., 2016; Li et al., 2017; Li et al., 2020; Bauer et al., 2002).

121 The Puy de Dôme (PUY) station is a reference site for the collection of cloud water from samples collected between  
122 2001 and the present. [Historically, the CWS sampler](#) has been widely used for microbial and chemical atmospheric  
123 studies at this site (Marinoni et al., 2004; Marinoni et al., 2011; Bianco et al., 2017; Joly et al., 2014). This model  
124 can collect wet or supercooled droplets, even at high wind speeds. It is made of aluminium or Teflon; the collection  
125 vessel can be removed for sterilisation and cleaning. However, the collected water volume of 10–60 mL per hour  
126 is a limit for chemical and microbial analyses that require increasing volumes. For long collection times, the vessel  
127 should be removed regularly to transfer the water into a sterile storage bottle. These manipulations expose the  
128 samples to contamination. The aspiration system must be powerful and, consequently, heavy and energy-  
129 consuming, which limits mobile sampling. The objective of this study was to present a ground-based cloud  
130 collector that responds to different constraints. This tool should be suitable for analysing cloud microbiology and  
131 chemistry, easy to clean and sterilise, allow the collection of high volumes of water, and be easy to deploy for field

132 campaigns (light and low energy consumption). To achieve these objectives, we developed [these last years](#) a  
133 collector [named BOOGIE](#). This study describes this instrument and compares it to other commonly used samplers  
134 to evaluate its efficiency.

## 135 **2 Materials and Methods**

### 136 **2.1 Conception of the BOOGIE cloud collector**

137 The 3D drawing was performed with Autodesk® Inventor 2016 and recently updated using the 2019 version. The  
138 prototype of the collector used in this study was fabricated on an aluminium stand (Al 5754 and 6060). This  
139 material exhibits robust properties and can be easily sterilised by autoclaving before field collection. Aluminium  
140 plates were cut using a laser and folded using a metal press. The collection funnel was adapted to a GL 45 thread  
141 to directly screw borosilicate glass or polytetrafluoroethylene (PTFE) bottles. All the aluminium parts were treated  
142 by QUANALOD® anodisation, with thickness of 20 µm, suitable for aluminium objects exposed to harsh  
143 environmental conditions. All parts were thoroughly cleaned to eliminate all manufacturing residue and several  
144 cycles of sterilisation by autoclaving (121°, 20 min per cycle) were performed to clean the collector.

145 The vacuum inside the collector was ensured by an axial fan (EMB-papst®, model 6300TD, S-Force, 40 W, 12 V  
146 DC) able to work under wet conditions and temperatures of -20 °C to 70 °C. It has a fan diameter of 172 mm and  
147 a [theoretical](#) maximum flow capacity of 600 m<sup>3</sup> h<sup>-1</sup> (manufacturer data). It is equipped with a controlled voltage  
148 for speed setting, which allows modulation of the fan velocity according to 10 increasing intensities. To measure  
149 the air inlet and outlet velocity, a thermal anemometer efficient from 0.2 to 20 m s<sup>-1</sup> was used (model Lutron AM-  
150 4204 from RS PRO®).

### 151 **2.2. Computational Fluid dynamics (CFD) simulations**

152 Finite element modelling and simulations were performed using Simcenter 3D software from Siemens Industry  
153 Software Inc., version 2022.1. The solver environment was Simcenter 3D Thermal/Flow Advanced Flow. The  
154 flow and particle tracking solvers are proprietary to Maya Heat Transfer Technologies. Other numerical  
155 computations and figures were performed using MATLAB version 2021a.

156 The fluid domain is represented by the inner volume of the collector. To compute a realistic flow inside the  
157 collector, it is necessary to consider the structure of the collector, which is composed of thin walls and metal plates,  
158 to enable air deflection and the collection of cloud water droplets. The Simcenter 3D software allows the generation  
159 of a volume or mesh directly from the boundaries of different parts of the collector; however, this method was  
160 unsuitable because of the thin inner walls. The fluid domain was built using successive Boolean subtractions by  
161 leaving a void in the right place, leading to a realistic geometry of the air volume (**Figure S1a**).

162 A finite element mesh was created using CTETRA4 solid elements. The element size was variable: the internal  
163 mesh size was set to 20 mm, whereas the element size was set to 24 mm on the rear faces next to the fan and to  
164 only 4 mm on the front face, allowing air deflection and the collection of droplets (**Figure S1b**). The total numbers  
165 of elements and nodes were 869 799 and 178 610, respectively.

166 For the air inlet flow, three slots of the collector front face were defined as the inlet flow boundary conditions. The  
167 flow direction was perpendicular to the front face and the external absolute pressure was equal to the ambient

168 pressure. For the air outlet flow, air velocity was applied to the rear circular face representing the fan. The  
169 magnitude varied according to the velocity ranges. The vector was perpendicular to the face.

170 The fluid is the standard air at the altitude of 1500 m (*i.e.*, summit of the PUY), at 15 °C, with the following  
171 physical characteristics: 1.1 kg m<sup>-3</sup> for the mass density and 1.75 kg m<sup>-1</sup> s<sup>-1</sup> for the dynamic viscosity.

172 The outlet velocity of the fan can be modulated among 10 intensities. The resulting air inlet volume flows have  
173 been measured using a hot-wire anemometer located in front of the slots. The surface area of the fan outlet was  
174 17671 mm<sup>2</sup>, and the total area of the three inlet slots was 10900 mm<sup>2</sup>. Therefore, there was a theoretical ratio of  
175 1.6 between the air inlet volume flow and the air outlet volume flows. To agree with the measured air inlet volume  
176 flow, the outlet velocities for the collector simulations were varied for the CFD simulations between 1 and 10 m  
177 s<sup>-1</sup> in 1 m s<sup>-1</sup> step.

178 Different particles were used in the simulation. The water drops were injected into the flow at the three air-inlet  
179 slots. Eight different values of drop diameter were selected between 5 and 20 µm. The water droplets were  
180 considered spherical. The drag coefficient was automatically calculated using the Reynolds number. The density  
181 of water was assumed to be 1 kg/dm<sup>3</sup>. Gravity was applied to the cloud particles, and the gravity vector was defined  
182 as the -Z axis with an acceleration amplitude of 9.81 m s<sup>-2</sup>. The sizes and masses of each particle class are  
183 summarised in **Table S1**.

184 In the air flow inside the collector, three vertical plates participated in droplet collection. If cloud water drops  
185 impact them, they should flow to the bottom of the funnel. Therefore, there is a specific surface configuration; if  
186 the water drops stick to the collection face, they do not rebound.

187 We selected the fully coupled pressure-velocity solver to solve the mass and momentum equations simultaneously  
188 for each time step. The solver iterates the pressure and velocity solutions until convergence is achieved at each  
189 time step. Modelling fluid flow turbulence is crucial for accurately simulating airflow. The flow solver uses  
190 different turbulence models that add a viscosity term to the Navier–Stokes governing equations. The two-equation  
191 model computes the viscosity term using two additional equations that are solved in parallel with the Navier–  
192 Stokes equations. Among the two-equation models, the k-omega [turbulence](#) model was selected for this study. The  
193 steady state time step was fixed to 0.01 s for all the model simulations.

194 For the steady-state simulation, the flow was fully developed, and its properties (velocity, pressure, and turbulence)  
195 were used in the particle-tracking equation. During the analysis, the software solved the equation of motion for  
196 each particle once per time step. Notably, because the particle tracking simulation is independent of the flow  
197 simulation, the particles do not affect the 3D flow. The injection duration in the fluid domain was 60 s, which is a  
198 good compromise between the relevant calculation and a reasonable simulation time.

## 199 **2.3 Experiments: inter-comparison of samplers**

### 200 **2.3.1 Sampling site**

201 The testing site of the different cloud collectors was the observatory of the PUY summit at 1465 m above sea level.  
202 It is part of the Cézeaux-Aulnat-Opme-Puy De Dôme (CO-PDD) instrument platform for atmospheric research  
203 (Baray et al., 2020). PUY is recognised as a global station in the Global Atmosphere Watch (GAW) network and  
204 is part of the European and national research infrastructures Aerosol Cloud and Trace Gases Research

205 Infrastructure (ACTRIS) and the Integrated Carbon Observing System (ICOS). The PUY is often located in the  
206 free troposphere, particularly during cloud events, and the characterised air is representative of synoptic-scale  
207 atmospheric composition. Various biological, physical, chemical, and cloud microphysical parameters were  
208 monitored on-site. For cloud microphysical properties, we use [the ground-based scattering laser spectrophotometer](#)  
209 [PVM-100](#) for cloud droplet volume measurements from Gerber Scientific, Inc. (Reston, VA, USA). [This](#)  
210 [instrument measures the laser light scattered in the forward direction by the cloud droplets. It allows to evaluate](#)  
211 [the particle volume density \(or LWC: liquid water content\) and the particle surface area density \(PSA\). The](#)  
212 [effective radius  \$R\_{\text{eff}}\$  can be calculated using LWC and PSA; it is an estimate of the average size of the cloud droplet](#)  
213 [population and does not represent the mean physical radius](#) (Guyot et al., 2015). All cloud microbiology and  
214 chemistry data are available in the PUYCLOUD database (<https://www.opgc.fr/data-center/public/data/puycloud>).

### 215 2.3.2 Cloud collectors

216 Two bulk cloud collectors were compared with a newly developed BOOGIE collector. These are active ground-  
217 based collectors commonly used in cloud field studies. They have different collection efficiencies, resulting in  
218 different volumes of cloud water that can be sampled. Cloud water collectors are generally designed to avoid the  
219 particles below 5 microns to avoid sampling the interstitial aerosol around the droplets. This is a compromise to  
220 obtain a sufficient volume of water with less contamination from dry and deliquescent particles. Typically, the  
221 smallest droplets were not sampled. The 50% collection efficiency cutoff, based on the droplet diameter, is often  
222 predicted from the impaction theory and strongly depends on the aerodynamic design of the impactor and the air  
223 flow rate (Berner, 1988; Schell et al., 1992). The collection efficiency for in situ conditions will depend on the  
224 LWC, and the meteorological conditions could strongly perturb the way the collectors are able to impact cloud  
225 droplets.

#### 226 *Caltech Active Strand Cloud water Collector: CASCC2*

227 A compact version of the original CASCC collector was used and lent by the Institut de Radioprotection et de  
228 Sûreté Nucléaire (IRSN). This sampler, named CASCC2, was constructed according to the recommendations of  
229 Demoz et al. (1996). It has an estimated cutoff diameter of 3.5  $\mu\text{m}$  (droplet diameter collected with 50% collection  
230 efficiency). [This collector has a metal body, stainless-steel collection strands, and a metal collection trough.](#) The  
231 airflow passed through a set of six rows of stainless-steel strings (diameter, 0.5 mm) with a velocity of 8.6  $\text{m s}^{-1}$ .  
232 The strings were vertically tilted 35°. The collector design has been shown to generate a stable airflow inside of  
233 348  $\text{m}^3 \text{h}^{-1}$ . [In Demoz et al. \(1996\), they proposed a correction to estimate the fraction of air that actually induces](#)  
234 [the sampling of the droplets; this was calculated to be 86%, resulting in a 299  \$\text{m}^3 \text{h}^{-1}\$  air flow.](#) The volume fraction  
235 of the ambient droplet distribution collected was evaluated in Demoz et al. (1996), who showed that this fraction  
236 is close to one over most of the LWC range (superior to 95%  $>0.1 \text{ g m}^{-3}$  of LWC). Therefore, at the end, a resulting  
237 sampled airflow at 284  $\text{m}^3 \text{h}^{-1}$  (4.73  $\text{m}^3 \text{min}^{-1}$ ) [could be estimated.](#) Cloud droplets coalesce on the strands and fall  
238 into a bottle through a Teflon tube owing to the combination of gravity and aerodynamic [drag](#). A description of  
239 the sampler is provided in **Figure S2**.

240 The collector body was stainless steel, the inlet contained the impaction rows, and the sample drainage was  
241 removed before each sampling for cleaning and sterilisation. A sterilised amber glass bottle was placed under the  
242 sample drainage during collection. [The CASCC2 was also not operated with a downward facing inlet allowing to](#)

243 [exclude the collection of rain](#). This cloud collector was not adapted for temperatures  $<0^{\circ}\text{C}$  because droplets freeze  
244 upon impact on metallic [strands](#). [Note that an upgraded version of the CASCC family was specifically designed](#)  
245 [for supercooled cloud sampling, the Caltech Heated Rod Cloud Collector \(CHRCC\)](#).

#### 246 *Cloud Water Sampler: CWS*

247 This collector (**Figure S3**) was developed specifically to collect warm and supercooled clouds, which can either  
248 freeze upon impact or be collected directly in the liquid phase (Kruisz et al., 1993; Brantner et al., 1994). It was  
249 designed to sample cloud water for specific studies on the detection for example of fungal spores and bacteria in  
250 cloud water (Tenberken-Pötzsch et al., 2000; Bauer et al., 2002). It comprises a single-stage impactor backed by a  
251 large wind shield (50 cm wide and 50 cm high) installed in front of the wind. The wind velocities were reduced in  
252 front of the shield, and the flow was directed into the single-slit nozzle. Cloud droplets ranging up to  $100\ \mu\text{m}$  in  
253 diameter were estimated to be stopped in front of the shield, stay airborne, and were sampled from a stagnant flow.  
254 Cloud droplets, which were drawn through a slit 25 cm long and 1.5 cm wide, collided on a rectangular aluminium  
255 collection plate installed horizontally, and water was collected in a reservoir below the plate. This sampler model  
256 presents an estimated cutoff diameter at 50% collection efficiency of  $7\ \mu\text{m}$  at a sampling rate of  $86\ \text{m}^3\ \text{h}^{-1}$ , as  
257 indicated in Brantner et al. (1994). The CWS used at the PUY was a homemade collector following the  
258 recommendation formulated by Kruisz et al. (1993); however, the suction system presented its own characteristics,  
259 with an inlet air velocity of  $13.5\ \text{m}\ \text{s}^{-1}$ . [As explained below for Boogie collector, inlet velocity measurement with](#)  
260 [hot-wire anemometer should be taken with care](#).

261 The blower was placed under the sampler and connected to the collector body via tubing. This was built of  
262 aluminium, and the collection plate and vessel were removable for cleaning and sterilisation. In contrast to the  
263 CASCC2, in which the water sample flowed into a glass bottle, in the CWS, the water remained in the collection  
264 vessel during the sampling period. It is not possible to check the collected volume during sampling, and the water  
265 must be regularly removed by opening the collector and transferring it to a storage bottle. This collector has been  
266 used for studies at PUY since the 2000s (Marinoni et al., 2004) because the collection plate and vessel can be  
267 sterilised in the laboratory, allowing for microbial analysis of cloud waters.

#### 268 **2.3.4 Chemical and microbial analysis**

269 Chemical and biological analyses were performed on the cloud samples following the standardised procedures  
270 described in Deguillaume et al. (2014). The main ions ( $\text{Cl}^-$ ,  $\text{NO}_3^-$ ,  $\text{NH}_4^+$ ,  $\text{SO}_4^{2-}$ ,  $\text{Na}^+$ ,  $\text{Ca}^+$ ,  $\text{Mg}^+$ ,  $\text{K}^+$ ) were analysed  
271 using ion chromatography. Formaldehyde and hydrogen peroxide levels were measured using derivatisation  
272 methods and analysed by fluorimetry. Total microbial cell counts, including bacterial, yeast, and fungal spores,  
273 were determined using flow cytometry. The microbial energetic state was determined by measuring ATP and ADP  
274 concentrations using bioluminescence. More information [on this analysis is given](#) in the Supplementary  
275 Information.

#### 276 **2.3.5 Back-trajectory analysis**

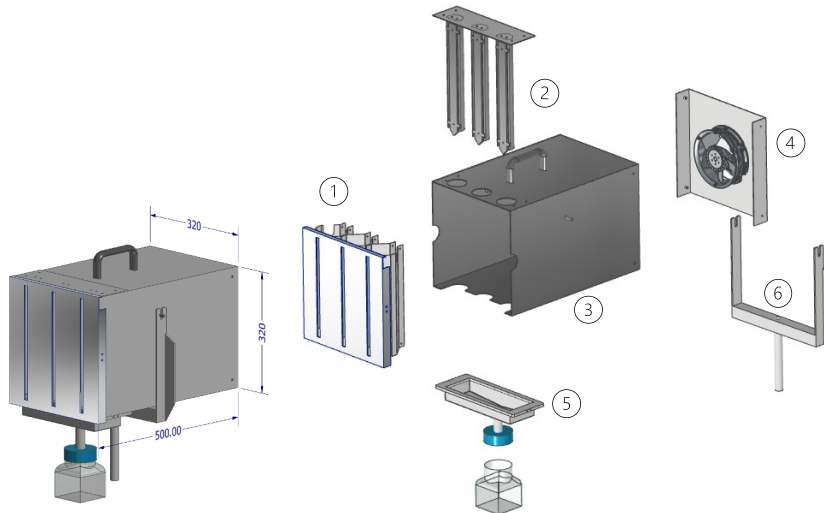
277 The CAT model (Baray et al., 2020) was used to estimate the air mass history reaching the summit of the PUY  
278 Mountain during the cloud-sampling period. This model uses the ECMWF ERA-5 wind fields and integrates a

279 topography matrix; back trajectories were calculated every hour during cloud sampling; the temporal resolution  
280 was 15 min, and the total duration was 72 h. These calculations are fully described by Renard et al. (2020).

## 281 3 Results

### 282 3.1 Conception and operating principles of the BOOGIE collector

283 The new collector is a single-stage collector that uses impaction to sample the cloud droplets (Marple and Willeke,  
284 1976). The collector is designed as a slit impactor. **Figure 1** shows the assembled collector (left) and the different  
285 parts of the collector and how they should be assembled for sampling. A GIF animation (**Movie 1**) showing the  
286 assembly of the collector before sampling is provided in the Supplementary Information. A photograph of the  
287 collector is shown in **Figure S4**, and all the dimensions are detailed in **Figure S5**. Parts 1, 2, and 5 were sterilised  
288 by autoclaving before sampling to allow for biological analysis.



289 **Figure 1. Schematic of the design of the BOOGIE collector. Assembly of the different parts of the BOOGIE collector:**  
290 **(1) front face with the three slots; (2) impaction plates; (3) collector body; (4) rear face with the fan; (5) funnel; (6)**  
291 **instrument holder.**  
292

293 The cloudy air entered via three rectangular inlets oriented vertically side by side, each 30 cm long and 1.2 cm  
294 wide, with 9 cm between them. The droplets were impacted by inertia on aluminium plates located 45 mm behind  
295 the air inlets. The inlet width and distance between the inlet and impaction plate were selected to be identical to  
296 those of the CWS. The air and smaller non\_collected droplets were directed to a shared corridor before the air fan.  
297 The collected water flowed to the collection funnel under gravity, and the collection bottle was sterilised.

### 298 3.2 Evaluation of the air flow inside the BOOGIE collector

299 The fan can be modulated at 10 intensities (10–100% of the maximum fan speed). Two ways have been  
300 investigated to calculate the air flow through the collector: either by measuring the air inlet velocities at the slots,



301 or by measuring the air outlet velocities. First, the air inlet velocities were measured in front of each of the three  
302 slots of the BOOGIE collector at different heights (high, middle, and low points), using a hot-wire anemometer,  
303 with the velocity modulated according to these 10 values (Figure S6). The measured velocities varied from 2 to  
304 approximately 15 m s<sup>-1</sup>, with an increase of approximately 1.5 m s<sup>-1</sup> per intensity step. The air inlet velocity  
305 stabilized at 90% of the fan speed (corresponding to a measured value of 14 m s<sup>-1</sup>). By positioning the anemometer  
306 identically at each measuring point, the measured velocities at different fan intensities were homogeneous between  
307 slots and for the same slot at different heights. However, the positioning of the anemometer is quite sensitive, since  
308 a slight displacement can lead to significant measurement deviations. This finding of air velocity heterogeneity at  
309 the slots will also be discussed in section 3.3.1.

310 Therefore, we designed an experiment to measure the air flow at the collector outlet. The airflow rate at the fan  
311 outlet was measured using the following procedure. A 3.5 m long PVC pipe with an internal diameter of 154 mm  
312 was installed after the fan outlet. This diameter enables the entire flow to be measured without reduction, thus  
313 limiting the additional pressure losses generated by the addition of the pipe. A hot-wire anemometer was installed  
314 in the tube at 3 m from the fan. The large distance/diameter ratio (greater than 19) minimizes disturbances (high  
315 turbulence and vortex rates) as the air passes through the axial fan.

316 The flow velocity profile is measured every 5 mm along the diameter. Flow rate is calculated by summing the  
317 average velocity for each ring by the ring area. The flow rate was estimated at 433 m<sup>3</sup> h<sup>-1</sup> at 90% of the fan speed.  
318 The average velocity in the pipe is found by dividing the flow rate by the cross-sectional area, which corresponds  
319 to a velocity of 6.5 m s<sup>-1</sup>. Based on this velocity, the Darcy-Weisbach formula and the Moody diagram (with a  
320 relative roughness of 2 · 10<sup>-5</sup>), the pressure drop in the pipe is estimated at 10 Pa. As a result, the addition of the  
321 pipe has little influence on the flow rate.

322 The pressure drop in the BOOGIE impactor can be estimated from the fan and flow characteristics. Since the flow  
323 rate has been calculated at 433 m<sup>3</sup> h<sup>-1</sup>, the pressure drop compensated by the fan is estimated at 220 Pa, and  
324 consequently the pressure drop in the impactor is around 210 Pa. The variation in density is less than 0.0025 kg  
325 m<sup>-3</sup>, i.e. a variation of less than 0.25%. The flow can be considered incompressible, and conservation of flow-  
326 volume can be used. The average velocity at the BOOGIE inlet is estimated at 11 m s<sup>-1</sup>, by dividing the flow by  
327 the inlet cross-section of 10.9 · 10<sup>-3</sup> m<sup>2</sup>. This average velocity differs from the measured velocity at inlet (14 m s<sup>-1</sup>)  
328 due to the velocity profile at the slots. The measurement corresponds to a maximum velocity.

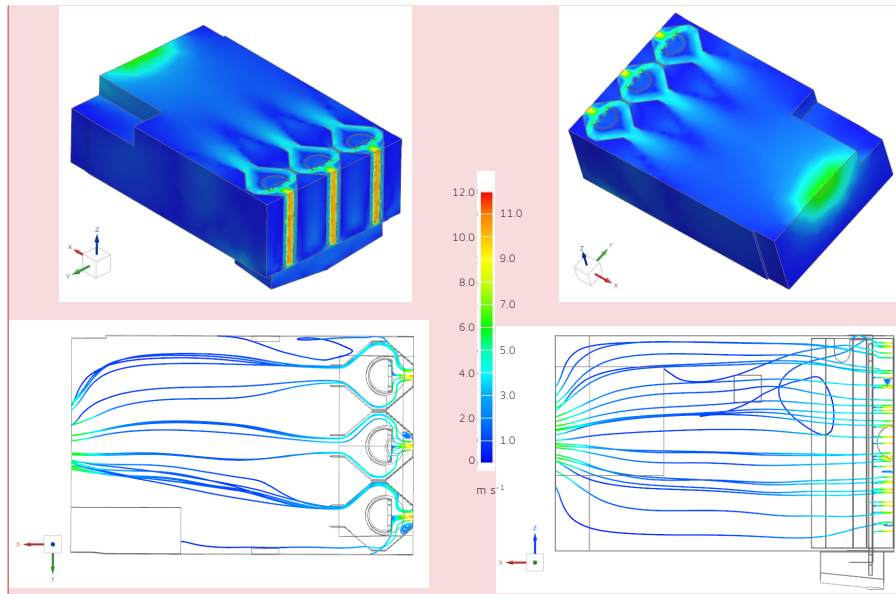
### 329 **3.3 Performance evaluation**

#### 330 **3.3.1 CFD simulations**

##### 331 *Flow velocity*

332 Several simulations were performed modulating the air outlet velocity from 2 to 10 m s<sup>-1</sup>. Use of air outlet velocity  
333 as boundary condition avoids imposing direction and velocity distribution at inlet. Figure 2a and b displays the  
334 flow velocity field inside the collector for air outlet flow velocity equal to 6.5 m s<sup>-1</sup> based on its experimental  
335 evaluation presented in section 3.2. (the same for 2 m s<sup>-1</sup> in Figure S7a and b). The air outlet flow velocity equal  
336 to 6.5 m s<sup>-1</sup> corresponds to a mean air inlet flow velocity equal to 11 m s<sup>-1</sup> (1.6 factor). Experimentally, we measured  
337 the air inlet flow velocity at a higher value around 14 m s<sup>-1</sup>. We present the horizontal cutting planes at the centre  
338 of the fan. Regardless of the air outlet velocity, the colour display of the flow velocity contour is identical. We can

339 notice that the velocity simulated close to the slots are heterogeneous confirming the difficulty of robustly  
340 measuring input speed.



342  
343 **Figure 2.** a) and b) Cutting plane in the flow velocity contour (in magnitude) in the case of an  $6.5 \text{ m s}^{-1}$  air outlet flow  
344 velocity; c) and d) set of streamlines in the collector (c- right view, d - top view) in the case of an  $6.5 \text{ m s}^{-1}$  air outlet flow  
345 velocity. Colour code indicates the different air velocity inside the collector.

346 Streamlines were also displayed (**Figures 2c and d and S7c and d**), with a set of seed points selected randomly  
347 on the air inlet faces. They displayed velocity results by showing the path taken by a massless particle. Each point  
348 along a streamline is always tangential to the velocity vector of the fluid flow. Again, the streamlines were only  
349 slightly modified between the two velocities.

#### 350 **Particle impact tracking**

351 Various **radius sizes** of particles were injected into the collector at different air outlet velocities. **Table S2** lists the  
352 number of water droplets for each air outlet velocity and each **size** of particles (**from 5 to 20  $\mu\text{m}$  in diameter**)  
353 recorded by the solver in front of the three inlets, represented by the three slots. Arbitrarily, approximately 60 000  
354 particles are injected. We calculated the number of injected droplets that impacted the vertical plates among the  
355 60 000 particles; this allowed **to calculate the normalized efficiency of particle collection for each size of particle**  
356 **and each velocity.** **Figure 3** reports the efficiency of collection in terms of the number of droplets and the mass of  
357 **the droplets.**

**Commenté [LD2]:** The figure is new since it corresponds to a  $6.5 \text{ m s}^{-1}$  simulation (air outlet flow)

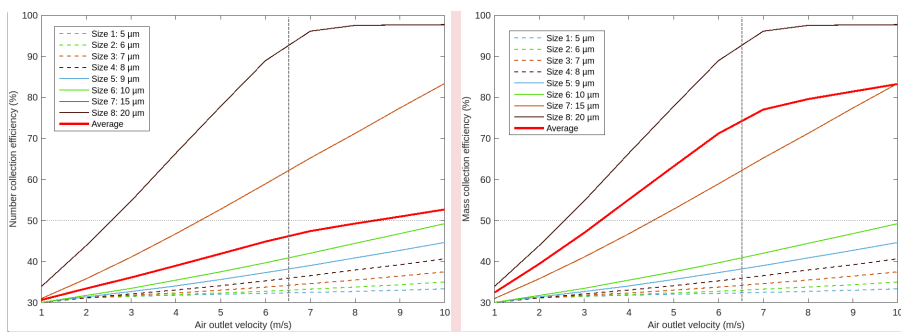


Figure 3. Normalized efficiency of the particle collection, regarding the number of droplets (a) and regarding the mass of the droplets (b) for different diameter size of particle.

We can observe that as the air outlet velocity increases, so does the collection efficiency for all droplet sizes. For sizes 7 and 8 (more than 15 μm in term of diameter), the number collection efficiencies were >50% for velocities superior to 4.5 m s<sup>-1</sup>. At higher speeds, number collection efficiencies >80% were achieved for both size classes. At the maximum speed, a collection efficiency of approximately 50% was reached for size 6 (10 μm in diameter). Considering the mass of the droplets, the two largest sizes (15 and 20 μm in diameter) naturally represented the largest mass of water collected. Because these two sizes were efficiently collected even at low air velocities, a collection efficiency of 50% in terms of mass was achieved at 3 m s<sup>-1</sup> of velocity. At 6.5 m s<sup>-1</sup> velocity, the average collection efficiency was approximately 75% and 47% in terms of mass and number, respectively.

At 6 m s<sup>-1</sup>, we observed a slowdown in the overall collection efficiency because the largest drops were already 100% collected. These results allowed us to estimate the theoretical cutoff diameter at approximately 12 μm when the air outlet velocity is 6.5 m s<sup>-1</sup>.

These results are subject to limitations and uncertainties related to the modelled physical phenomena. First, the statistical results from the CFD simulations were based on a certain number of particles injected into the computational domain to achieve reasonable computing times. Second, the collection surfaces are supposed to be "ideal": a droplet, that impacts a plate, sticks to it; therefore, its transport by gravity to the funnel remains hypothetical. Third, none of the physical phenomena were considered; the simulations were based on the equations of classical fluid mechanics, but other phenomena, such as electrostatics or Brownian motion, may affect the lightest particles. And last, we can also mention that the air outlet velocity estimated experimentally is also subject to uncertainties that could impact the evaluation of the cutoff diameter. However, the performed simulations indicate that the new BOOGIE collector is able to collect cloud droplets, which also confirms that the distance between the air inlet slots, and the outlet fan is adequate because it is beneficial for air flow stabilisation.

### 3.3.2 Field sampling experiments

To evaluate the performance of the BOOGIE sampler, 21 cloud events were collected at PUY station over the period 2016-2024 and the collected water mass as a function of the sampled volume of air was measured (Wieprecht et al., 2005; Demoz et al., 1996). In our database, we selected these events based on the availability of LWC measurements and of the measured mass of the collected water. Table S3 reports various parameters measured during the sampling duration: meteorological parameters (temperature and wind speed) and

Commenté [LD3]: The figure is corrected (legend, axis etc.)

a supprimé: On average, for all droplet sizes, the average collection efficiencies of >50% in terms of numbers were achieved at air velocities >8 m s<sup>-1</sup>.

a supprimé: The results highlight that the collector should be used with the highest velocity because the collection efficiency is theoretically maximal. However, at

a supprimé: , which represented the diameter at which 50% of the drops were collected. In our case, for the simulation conditions, this can be estimated

a supprimé: from May to July 2016 and from July to November 202

a supprimé: . Seventeen To evaluate the cloud events, corresponding to twenty samples, were collected using BOOGIE to evaluate its collection performance, by measuring

403 microphysical cloud properties (Liquid Water Content  $LWC_{meas}$ , and effective radius,  $R_{eff}$ , every 5 min). These  
404 cloud events were in warm conditions between -1 to 11 °C with moderate wind speed (0.2 to 16 m s<sup>-1</sup>) and a LWC  
405 from 0.11 to 0.71 g m<sup>-3</sup>. In 2021, 3 cloud events were collected using two BOOGIE collectors deployed in parallel  
406 (corresponding to S1 and S2 samples). In 2024, the collection with two collectors was systemically done and  
407 several samples were collected consecutively during 4 cloud events (15/04/2024, 25/04/2024, 26/04/2024 and  
408 29/04/2024). At the end, 39 samples were used to estimate the BOOGIE collector.

409 First, we can estimate the cloud water collection rates of BOOGIE equal to  $100 \pm 53$  mL h<sup>-1</sup>. Water volume is  
410 crucial because it determines the biological and chemical analyses that can be performed in the laboratory. The  
411 BOOGIE collection rate allows sufficient cloud water to be obtained in a short duration, which is crucial because  
412 the origin of the air mass that reaches the collection site can vary in a short time.

413 Experimentally, we can also evaluate the Collected LWC ( $CLWC_{exp}$ ) in g m<sup>-3</sup> (Waldman et al., 1985) as:

414 
$$CLWC_{exp} = \frac{M}{F \times \Delta t} \quad (1)$$

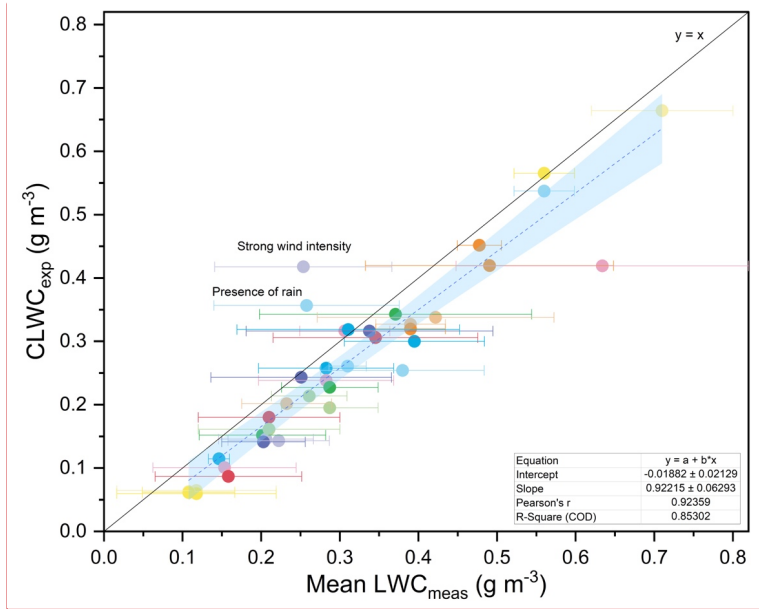
415 where M is the collected water mass (g); F is the sampler airflow (m<sup>3</sup> min<sup>-1</sup>); and  $\Delta t$  is the sampling duration (min).

416 To evaluate  $CLWC_{exp}$ , we estimated in section 3.2, the sampled air flow experimentally at 433 m<sup>3</sup> h<sup>-1</sup> (7.22 m<sup>3</sup>  
417 min<sup>-1</sup>). In this calculation, we were not able to distinguish the fraction of the air that induced the impaction of  
418 droplets as evaluated for the CASCC2 by Demoz et al. (1996).

419  $CLWC_{exp}$  can be compared with the measured mean  $LWC_{meas}$  for the 21 cloud events (i.e., 39 samples), as shown  
420 in **Figure 4**.

**a supprimé:** The optimal simulated collection efficiency for this collector was simulated for an outlet air velocity equal to 8 m s<sup>-1</sup> corresponding to a theoretical inlet air velocity of 12.8 m s<sup>-1</sup> (Section 3.2.1).

**a supprimé:** For cloud-water sampling, the sampler was operated at its maximum inlet air velocity. Using a thermal anemometer directly in front of the slots, we measured an air velocity of 14 m s<sup>-1</sup> (Section 3.1); therefore, we can estimate the outlet velocity at 8.75 m s<sup>-1</sup>. To calculate the volume of the sampled air, we use this value for the outlet air velocity; thus, the sampled air flow can be evaluated as follows: with three inlets of 302 mm length and 12 mm width giving a total inlet surface of  $10.9 \times 10^{-3}$  m<sup>2</sup> and an air velocity of 8.75 m s<sup>-1</sup>, then the airflow is 343.3 m<sup>3</sup> h<sup>-1</sup> (5.72 m<sup>3</sup> min<sup>-1</sup>).



**Commenté [LD4]:** The figure is new: the CLWC<sub>exp</sub> of all samples have been recalculated; new samples have been implemented; for the linear fit, we do not force the intercept at 0.

435  
436 **Figure 4.** Collected cloud water content CLWC<sub>exp</sub> vs measured LWC<sub>meas</sub> (in g m<sup>-3</sup>) for a selection of 21 cloud events  
437 samples at the PUY station. **The standard deviation of the measured LWC is indicated.** The black solid line represents  
438 the  $y = x$  function; linear fit of the experimental data is represented by the dotted blue line and the blue area denotes  
439 the 95% confidence interval of this fit.

440 The CLWC<sub>exp</sub> and measured LWC<sub>meas</sub> were well correlated (the slope of the linear regression was 0.92, and the  
441 intercept was  $-0.02 \text{ g m}^{-3}$ ). Systematic and random deviations from the “theoretical” efficiency are represented by  
442 a 1:1 line. Among the 23 cloud samples, only 2 cloud events presented a CLWC<sub>exp</sub> significantly higher than the  
443 LWC<sub>meas</sub>. **Explanations can justify this bias: the cloud event collected the 3/04/2024 present high wind speed with**  
444 **a period during the sampling (20 min) where it reached  $16 \text{ m s}^{-1}$  and the cloud event sampled the 29/04/2024 was**  
445 **characterized by the presence of a fine rain at the end of the sampling period.**

446 The sampling efficiency can be estimated as follows:

447 
$$\text{Sampling efficiency (\%)} = \frac{\text{CLWC}_{\text{exp}}}{\text{LWC}_{\text{meas}}} \times 100 \quad (2)$$

448  
449 The average calculated sampling efficiency over 21 cloud events was equal to  $73.9 \pm 21.4 \%$ . **Without considering**  
450 **the two cloud events with significant overestimation of CLWC<sub>exp</sub> vs LWC<sub>meas</sub>, the sampling efficiency falls to**  
451  **$69.7 \pm 11\%$ .** The sampling efficiency **does not** appear to decrease when there was a shift to higher LWC<sub>meas</sub>. **This**  
452 **phenomena has been observed** with other samplers such as the CASCC2, possibly explained by interior collector  
453 wall losses for large droplets (Wicprecht et al., 2005).

454 The mean cloud wind speed and effective cloud droplet radius varied between the cloud events. **Figure S8** shows  
455 the sampling efficiency vs the three meteorological and microphysical parameters. The 21 clouds were sampled  
456 under conditions typically encountered at PUY for cloud sampling under warm conditions and for different

457 seasons: minimal temperatures  $> -1$  °C with a maximum value of approximately 11 °C; wind speed varying from  
458 0.2 to 16 m s<sup>-1</sup>. No tendency was observed between the sampling efficiency and temperature, supporting the fact  
459 that the collector can be operated over different seasons. The collector's orientation towards the wind is important,  
460 particularly under strong wind conditions. Incorrect orientation (*i.e.*, not in front of the wind) could drastically  
461 reduce collection efficiency, whereas orientation towards strong winds could improve collection efficiency. For  
462 the collected cloud events, we observed that the collection efficiency slightly increased with wind speed; however,  
463 the strength of the association was small. At high wind speeds (gusts) near 10 m s<sup>-1</sup>, cloud droplet sampling can  
464 be non-isokinetic, explaining the possible perturbation of collection efficiency. We can notice that 4 cloud events  
465 (corresponding to 6 samples) were collected during high wind condition (more than 11 m s<sup>-1</sup>). A problem with the  
466 orientation of the collector in strong wind condition can lead to significant gaps in collection efficiency. We cannot  
467 rule out the possibility that at some point the collector may not face the wind, leading to a reduction in collection  
468 efficiency, or that it may face the wind at very high intensities, leading to sampling in non-isokinetic conditions  
469 and inducing collection efficiencies more than 100%. This is clearly seen in these 4 events, which show highly  
470 heterogeneous collection efficiencies (from 63.5 to 164.7%). The average effective radius varied from 4.6 to 12  
471 μm; there was no correlation between this parameter and the collection efficiency, indicating adequate collection  
472 performance of the collector even for smaller droplets.

473 The collection efficiency calculated herein uses the theoretical total cloud water based on integrated measurement  
474 methods (LWC). These estimates must be treated with caution because they are marred by several  
475 errors/approximations listed here. These can be the result of the limitations of the instruments themselves (the  
476 collector and the PVM probe) and the sampling conditions (wind); with the PVM-100 probe, we cannot optimally  
477 capture the time evolution of the LWC because data are recorded every 5 min. Finally, the theoretical sampler  
478 airflow used to calculate CLWC<sub>exp</sub> can be additionally perturbed by the wind condition. Nevertheless, this first  
479 comparison provides a rough estimate of the collection performance of the BOOGIE collector, which appears to  
480 be suitable for contrasting environmental conditions.

### 481 **3.4 Comparison of cloud samplers**

482 A field campaign was conducted at PUY in 2016 to compare the new collector with other commonly used samplers.  
483 The BOOGIE collector has been deployed to sample clouds together with the CWS used at the PUY station since  
484 2001 and the CASCC2 (**Figure S9**). From 1<sup>st</sup> June to 2<sup>nd</sup> July, four cloud events were simultaneously collected  
485 using these three samplers. The meteorological conditions and microphysical cloud properties were monitored  
486 during the cloud events (**Figure S10**). Back trajectories were computed using the CAT model for the four cloud  
487 events (**Figure S11**). The three samplers were oriented in front of the wind at the beginning of the sampling period;  
488 changes in the wind direction were checked during this period, and the orientation of the collectors was modified  
489 accordingly.

490 The prevailing winds during the first two cloud events (01 and 04/06/2016) arrived from the north-northwest and  
491 north-northeast directions, whereas the other two (28/06/2016 and 02/07/2016) were locally associated with winds  
492 coming from the southwest direction. This last event was also characterized by strong wind speeds of up to 14 m  
493 s<sup>-1</sup> at the end of the sampling time. For the four cloud events, the wind directions did not drastically change during  
494 the sampling duration except for on the 4<sup>th</sup> June where some fluctuations were observed; however, these were not  
495 significant because the wind speed was extremely low (0.2 m s<sup>-1</sup>). Regarding the microphysical properties, the first

496 cloud event presented lower mean measured LWC ( $0.15 \text{ g m}^{-3}$ ) in comparison to the others (approximately  $0.3 \text{ g}$   
 497  $\text{m}^{-3}$ ). In contrast, the average radius was highest for the first cloud event (10.8 vs 4.5–6.6  $\mu\text{m}$  in radius). The  
 498 temperature corresponded to warm cloud conditions (between 6 and  $10 \text{ }^\circ\text{C}$ ), allowing the collection of liquid  
 499 droplets.

### 500 *Sampling efficiency*

501 First, the cloud water samplers were compared in terms of sampling efficiency, considering the calculated  
 502  $\text{CLWC}_{\text{exp}}$  and measured  $\text{LWC}_{\text{meas}}$  (equation (2)). For the CASCC2, the airflow was evaluated following Demoz  
 503 et al. (1996) (Section 2.3.2). In the calculation presented below, we decided to use the value  $348 \text{ m}^3 \text{ h}^{-1}$  without  
 504 distinguishing the fraction of “sampled air” from the total air entering the collection system. We motivate this by  
 505 the fact that with the two other collectors we are not able to estimate this fraction. This will allow to compare  
 506 collection efficiencies estimated on the same calculation basis. The sampled airflow was evaluated for the CWS,  
 507 which is a homemade collector that follows the recommendations of Kruisz et al. (1993). As indicated in Section  
 508 2.3.2, the air inlet flow velocity was measured with a hot-wire anemometer as  $13.5 \text{ m s}^{-1}$ . Therefore, considering  
 509 the surface of the entry slot, the sampled air entering the CWS collector was calculated to be equal to  $182 \text{ m}^3 \text{ h}^{-1}$   
 510 ( $3.04 \text{ m}^3 \text{ min}^{-1}$ ). We are aware that this estimation is rough since, as for the BOOGIE collector, the measurement  
 511 of the air flow velocity at the slot entry is difficult since the positioning of the probe induces biases in the  
 512 measurement.

513 **Table 1. Information on cloud water collection performed with BOOGIE, CWS and CASCC2 samplers for four**  
 514 **independent cloud events at PUY. The temperature, wind speed and  $R_{\text{eff}}$  are averaged over the sampling time.**

Cloud events: duration, mean temperature, mean wind speed & mean effective radius	Sampler	BOOGIE	CWS	CASCC2
	Airflow ( $\text{m}^3 \text{ h}^{-1} / \text{m}^3 \text{ min}^{-1}$ )	<u>433/7.22</u>	<u>182.2/3.04</u>	<u>348/5.8</u>
Date = 01/06/2016	$\text{LWC}_{\text{meas}}$ ( $\text{g m}^{-3}$ )		$0.15 \pm 0.01$	
Duration = 90 min	Sampled volume of air	<u>650</u>	<u>273</u>	<u>522</u>
$T = 6.3 \pm 0.2 \text{ }^\circ\text{C}$	Collected water (g)	59	19	40
Wind speed = $8.1 \pm 0.5 \text{ m s}^{-1}$	$\text{CLWC}_{\text{exp}}$ ( $\text{g m}^{-3}$ )*	<u>0.09</u>	<u>0.07</u>	<u>0.08</u>
$R_{\text{eff}} = 10.8 \pm 0.7 \mu\text{m}$	Sampling efficiency (%)*	<u>62</u>	<u>47</u>	<u>54</u>
Date = 04/06/2016**	$\text{LWC}_{\text{meas}}$ ( $\text{g m}^{-3}$ )		$0.31 \pm 0.06$	
Duration = 180 min	Sampled volume of air	<u>1299</u>	<u>545</u>	<u>1044</u>
$T = 7.8 \pm 0.2 \text{ }^\circ\text{C}$	Collected water (g)	326	110	261
Wind speed = $0.3 \pm 0.1 \text{ m s}^{-1}$	$\text{CLWC}_{\text{exp}}$ ( $\text{g m}^{-3}$ )*	<u>0.251</u>	<u>0.202</u>	<u>0.250</u>
$R_{\text{eff}} = 6.6 \pm 0.6 \mu\text{m}$	Sampling efficiency (%)*	<u>84</u>	<u>66</u>	<u>82</u>
Date = 28/06/2016	$\text{LWC}_{\text{meas}}$ ( $\text{g m}^{-3}$ )		$0.35 \pm 0.13$	
Duration = 60 min	Sampled volume of air	<u>433</u>	<u>182</u>	<u>348</u>
$T = 9.3 \pm 0.14 \text{ }^\circ\text{C}$	Collected water (g)	105	34	88
Wind speed = $2.3 \pm 0.4 \text{ m s}^{-1}$	$\text{CLWC}_{\text{exp}}$ ( $\text{g m}^{-3}$ )*	<u>0.243</u>	<u>0.187</u>	<u>0.253</u>
$R_{\text{eff}} = 4.6 \pm 1.0 \mu\text{m}$	Sampling efficiency (%)*	<u>71</u>	<u>54</u>	<u>73</u>
Date = 02/07/2016	$\text{LWC}_{\text{meas}}$ ( $\text{g m}^{-3}$ )		$0.26 \pm 0.05$	
Duration = 360 min	Sampled volume of air	<u>2599</u>	<u>1091</u>	<u>2088</u>
$T = 9.7 \pm 1 \text{ }^\circ\text{C}$	Collected water (g)	440	135	290

**a supprimé:** Because the CWS and BOOGIE collectors have the same geometry as the impaction system, we applied the ratio (1.6) evaluated for the BOOGIE collector to calculate the outlet velocity ( $8.43 \text{ m s}^{-1}$ ).

**a supprimé:** estimated

**Commenté [LD5]:** In this table, all the data are new since we re-evaluated the air flow of the samplers. This is now explained above.

Wind speed = $12.0 \pm 1.5 \text{ m s}^{-1}$	CLWC <sub>exp</sub> (g m <sup>-3</sup> )*	0.169	0.124	0.139
Reff = $6.1 \pm 0.7 \mu\text{m}$	Sampling efficiency (%)*	65	48	54

\* The collected LWC (CLWC<sub>exp</sub>) is calculated following equation (1) and the sampling efficiency by equation (2); \*\* Fine raining event before the end of sampling.

520 The CASC2 and BOOGIE samplers collected **between 348 to 433** m<sup>3</sup> of air per hour, whereas the sampled  
521 volume of air collected by the CWS was markedly lower (**around 180** m<sup>3</sup> h<sup>-1</sup>), which explains the lower amount of  
522 collected water. The BOOGIE sampler presented a mean water collection rate for the four cloud events of  $82 \pm 32$   
523 mL h<sup>-1</sup>. **This** was significantly higher than **the rates obtained with** the other collectors (CASC2:  $62 \pm 30$  mL h<sup>-1</sup>;  
524 CWS :  $26 \pm 11$  mL h<sup>-1</sup>) (t-test, p<0.05). On average, the calculated sampling efficiencies were **70 ± 10%**, **53 ± 9%**,  
525 and **66 ± 14%** for BOOGIE, CWS, and CASC2, respectively. Overall, the three collectors exhibited similar and  
526 satisfactory collection efficiencies. **v**

527 **Wieprecht et al. (2005) highlighted that the CASC2 collection efficiency could be impacted by** the loss of droplets  
528 off the strands and/or losses inside the collector on the walls, as highlighted by particularly for large droplets. This  
529 collector appeared to be more affected by the intensity of wind speed, with the lowest collection efficiencies  
530 observed for the two windier cloud events. As reported by Krusiz et al. (1992) for CWS and shown in this study  
531 for BOOGIE, no correlation of wind speeds to the CLWC<sub>exp</sub> of the samplers was found. In the case of the 4<sup>th</sup> June  
532 cloud, the appearance of fine rain during sampling could possibly explain the **higher** collection efficiency observed  
533 for all collectors, as we did not observe conditions such as strong winds that could disrupt the sampling.  
534

535 Concerning the CASC2, a sampling efficiency was previously determined during the FEBUKO experiments in  
536 the Thüringer Wald (Germany) at  $56 \pm 17\%$  (Wieprecht et al., 2005). **This sampling efficiency for the CASC2**  
537 **seems to be slightly lower than that calculated in the present study.** Krusiz et al. (1993) calculated a sampling  
538 efficiency of approximately 60% for the CWS during sampling experiments performed at Mount Sonnblick  
539 (Austria) **in the same range of order than in the present study. The sampling efficiency depends on** environmental  
540 conditions and cloud microphysical properties, which differ between collection sites, **explaining this variability.**  
541 The four cloud events have also been sampled at PUY under “optimal” conditions (summertime conditions with  
542 limited wind speed and sufficient cloud LWC), possibly explaining the efficient collection of the samplers.

#### 543 **Cloud water chemical and biological composition**

544 To compare the three cloud water collectors, we also focused on the chemical compositions of the three cloud  
545 water samples collected in 2016. The concentrations of inorganic ions in samples collected with the CWS and  
546 CASC2 collectors (**Table S4, Figure S12**) were compared to the concentrations measured in samples collected  
547 with BOOGIE using the discrepancy factor (D<sub>f</sub>) calculated using **equations 3a and 3b.**

$$548 D_{f,CWS} = \frac{C_{BOOGIE} - C_{CWS}}{\frac{C_{BOOGIE} + C_{CWS}}{2}} \quad (3a)$$

$$549 D_{f,CASC2} = \frac{C_{BOOGIE} - C_{CASC2}}{\frac{C_{BOOGIE} + C_{CASC2}}{2}} \quad (3b)$$

550 where C<sub>BOOGIE</sub> is the concentration of ions measured in samples collected with BOOGIE, and C<sub>CWS</sub> and C<sub>CASC2</sub>  
551 are the concentrations of ions measured with CWS and CASC2, respectively.

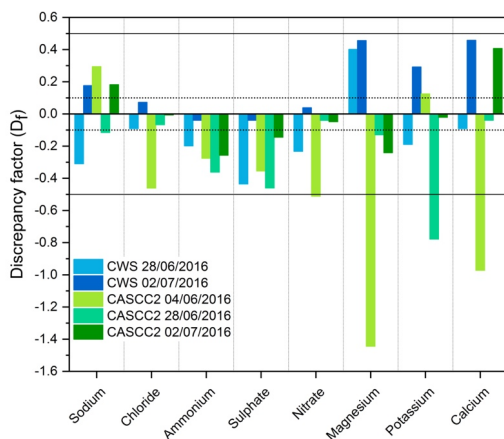
**a supprimé:** This confirms that the volume of water collected by cloud samplers could be used as a first approximation a proxy to estimate cloud LWC.



555 **Figure 5** shows the estimated  $D_{f,CWS}$  and  $D_{f,CASCC2}$  for anions and cations for cloud samples. The horizontal dashed  
 556 lines represent the analytical error on the measurement, which is comparable with  $D_{f,CWS}$  02/07/2016 for sulphate,  
 557 nitrate, chloride, and ammonium and  $D_{f,CASCC2}$  28/06/2016 and 02/07/2016 for nitrate, sulphate, chloride, and  
 558 sodium. The other  $D_f$  values were higher, but generally  $<0.5$ , which could represent a good comparability of the  
 559 cloud collectors, because the chemical composition of cloud condensation nuclei may be inhomogeneous. [A high](#)  
 560 [variability by a factor 3 to 6 was observed for the magnesium and potassium ions, but they also present a lower](#)  
 561 [concentration under 15 and 8  \$\mu\text{M}\$ , respectively \(Figure S12\). For the most concentrate ions as ammonium \(over](#)  
 562 [150  \$\mu\text{M}\$ \) and nitrate \(over 50  \$\mu\text{M}\$ \), their concentrations are comparable between the samplers.](#)

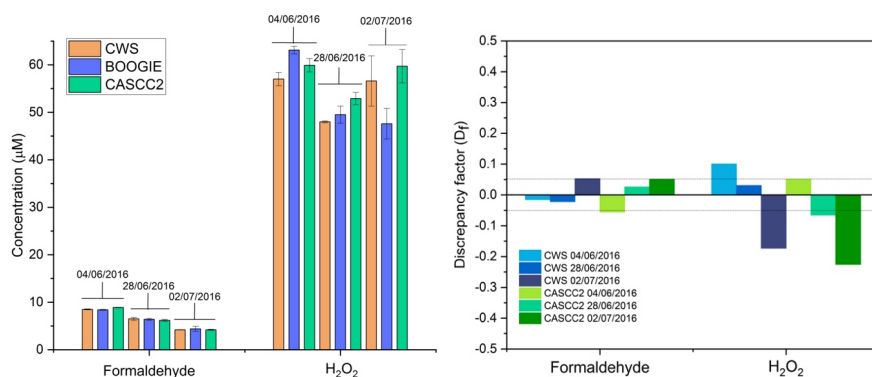
563 At first glance, concentrations with the CASCC2 appear to be slightly higher, but not for all ionic species and not  
 564 for all the cloud events. These three samplers present specific designs and surfaces of collection (plate for BOOGIE  
 565 and CWS vs strands for CASCC2), leading to different estimated cutoff diameters (12  $\mu\text{m}$  for BOOGIE, 7.5  $\mu\text{m}$   
 566 for CWS, and 3.5  $\mu\text{m}$  for CASCC2) and possibly to differences in the chemical composition of the samples.

567



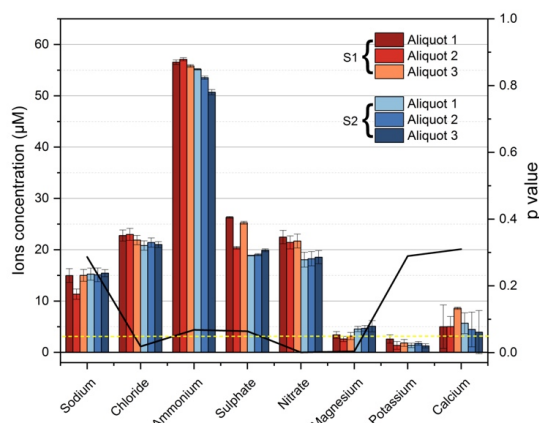
568  
 569 **Figure 5. Histograms presenting discrepancy factors ( $D_f$ ) between BOOGIE and CWS and CASCC2 calculated using**  
 570 **anion and cation concentrations for the three cloud samples. The dashed lines represent the analytical error, whereas**  
 571 **the plain line represents the 50% discrepancy.**

572 Formaldehyde and hydrogen peroxide concentrations have been also measured in samples obtained with the three  
 573 collectors. Concentrations and discrepancy factors between collectors are presented in **Figure 6**. These results are  
 574 consistent with what was observed with the ionic content because the collectors indicate  $D_f$  values mostly within  
 575 the analytical error and maximum measured  $D_f$  values  $<0.5$ .



576 **Figure 6. Left: Histograms presenting the formaldehyde and hydrogen peroxide concentrations for the three cloud**  
 577 **samples collected using CWS, BOOGIE, and CASC2 in parallel. The error bars correspond to the standard deviation.**  
 578 **Right: Histograms presenting discrepancy factors ( $D_f$ ) between the BOOGIE and CWS and CASC2. The dashed lines**  
 579 **represent the analytical error.**

580 To further evaluate BOOGIE, two identical collectors were installed at the PUY station in 2021 to check for  
 581 differences in the chemical composition of cloud waters collected in parallel. For clouds on 08/07/2021, chemical  
 582 measurements were performed in triplicate to analyze the statistical differences (**Figure 7, Table S5**). The error  
 583 bars depict the analysis error, which is higher than the discrepancy between the BOOGIE collectors for sodium,  
 584 potassium, calcium, and chloride. The black plain line represents the p-value obtained for the t-test (right y-axis);  
 585 if the p-value is  $<0.05$ , represented in the plot by the yellow dashed line, the difference between the two BOOGIE  
 586 collectors is significant, as observed for magnesium, nitrate, and chloride. Nevertheless, the difference was not  
 587 significant for sodium, ammonium, potassium, calcium, and sulphate, indicating good reproducibility of sampling  
 588 with the BOOGIE collectors.



589 **Figure 7. Histograms presenting the concentrations for a specific cloud sampled on 08/07/2021 at PUY with two**  
 590 **BOOGIE collectors. This time, three aliquots were analysed twice (error bars) using ion chromatography. p-values are**  
 591 **indicated with the black line and the yellow dashed line indicates the threshold of  $p = 0.05$ .**

**Commenté [LD6]:** Following the reviewer comment, we added in the manuscript this figure that was previously in the supplementary information.

592 Given the uncertainties in laboratory measurements and the possible intrinsic variability of the chemical  
 593 composition within the cloud system, we can reasonably argue that the chemical compositions of the collectors  
 594 are comparable. Schell et al. (1992) compared two single-stage cloud impactors with different designs and  
 595 highlighted the large differences between the ionic compositions of the samples. These differences have been  
 596 discussed to be related to different microphysical properties of the sampled clouds that induced bias in the  
 597 collection: smaller droplets can be sampled with a lower cutoff diameter of the collector, and a lower LWC can  
 598 eventually induce some evaporation of the smaller droplets. The three cloud events presented “stable”  
 599 microphysical properties during their collection period (Figure S9). This could explain the good agreement  
 600 between the collectors in terms of their chemical composition. Wieprecht et al. (2005) compared the chemical  
 601 composition of cloud water collected with a low-volume single-stage slit jet impactor and with the CASCC2 string  
 602 collector and reported 8–15% differences in the solute ionic mass in cloud water, in the range observed in the  
 603 present study (4–35% of differences, average of 12%) between the three collectors.

604 The microbial energetic state given by the in-cell ATP and ADP concentrations from each cloud sample was  
 605 assessed during the inter-comparison campaign (see Supplementary Information for a description of the protocol).  
 606 The ATP/ADP ratio gives the energetic stress of the cloud water microbiota; a ratio  $<0.6$  indicates a good energetic  
 607 state, 0.6 to 1, a medium one, and  $>1$ , a low energetic state. The measured ratios are listed in Table S6. The  
 608 ATP/ADP ratio ranged from 0.2 to 0.4, revealing a good energetic state of microflora for each sample. The  
 609 measured ATP/ADP ratios were similar for the cloud water samples from the three collectors. Thus, we argue that  
 610 the three samplers could be considered non-stressful and suitable for cloud microbiota collection.

#### 611 4 Conclusions

612 This study presented a new cloud collector called BOOGIE. This single-stage collector allows cloudy air  
 613 containing aqueous droplets to be drawn through three air inlets in the form of vertically oriented slots. The cloud  
 614 droplets were collected using vertical plates placed behind the slots, allowing them to be impacted. They then

615 flowed by gravity along the plates, fell into a funnel, and ended up in a sterilised glass bottle. It was made of  
616 aluminium, but can be manufactured from other materials, such as plastic materials such as nylon or PTFE to  
617 investigate transition metal ions in cloud waters. The cloud collector can be connected to the mains or run on  
618 batteries (12 V voltage); thus, the collector can be operated at its own power during field measurement campaigns  
619 for at least 4 h using a 2 kg small battery. Parts of the sampler were removed for cleaning; the front face, impaction  
620 chamber, funnel, and glass bottle were sterilised in an autoclave. This allowed for the characterisation of the  
621 biological content of the sampled clouds (biodiversity, concentration, and viability/activity) (Vařtilingom et al.,  
622 2012). Biological and chemical collector blanks were easily prepared by spraying MilliQ water onto the collection  
623 plates and collecting the water flowing into the collection glass bottle.

624 CFD simulations were performed to investigate how the collector captured cloud droplets. First, considering the  
625 3D-dimensional structure of the collector, some turbulences were simulated inside the collector, which was  
626 reassuring. Different sizes of cloud droplets were injected into the collector to simulate their impacts on the  
627 collection plates. This theoretical study indicates that on average, for all droplet sizes (radius from 2.5 to 10  $\mu\text{m}$ ),  
628 the average collection efficiencies of  $>50\%$  in terms of numbers were achieved at air outlet velocities  $>8\text{ m s}^{-1}$ . A  
629 collection efficiency of approximately 50% was reached for 5  $\mu\text{m}$  droplets in radius that gave us an estimate of the  
630 50% cutoff diameter of the collector (approximately 12  $\mu\text{m}$ ). This estimate seems higher than the cutoff diameters  
631 of other cloud samplers (more in the range between 3.5 and 10  $\mu\text{m}$  in diameter). However, comparisons of cutoff  
632 diameters between samplers are difficult because these estimates are made using different methods; in particular,  
633 the theoretical collection efficiency often considers the Stokes number (Demos et al., 1996).

634 Based on the 21 cloud events sampled at the PUY station, a mean water collection efficiency was calculated as  
635 100 + 53 mL h<sup>-1</sup> for clouds presenting various microphysical cloud properties: the mean LWC was between 0.11  
636 and 0.71  $\text{g m}^{-3}$  and the mean effective radius  $R_{\text{eff}}$  was between 4.6 and 11.8  $\mu\text{m}$ . This made it possible to obtain  
637 sufficient water volumes over short periods for targeted chemical and biological analyses. This is crucial for  
638 minimally integrating the cloud properties in space and time. Methodological developments in recent years have  
639 made it possible to assess the organic composition and biodiversity of this aqueous environment using non-targeted  
640 methods (Rossi et al., 2023; Bianco et al., 2018). This requires large volumes of cloud water (hundreds of milliliters  
641 or even liters of water), which can be collected rapidly using the new collector alone or by duplicating it.

642 Considering the measured LWC,  $\text{LWC}_{\text{meas}}$ , the sampling efficiency of this new collector was estimated at 69.7 +  
643 11% over the same set of cloud events collected at PUY. No significant tendency in the collection efficiency was  
644 observed as the wind speed increased, over the range of variation between 0.3 to more than 15 m s<sup>-1</sup> and definite  
645 variability in the collection efficiency was observed at high wind condition. No significant correlation was  
646 observed between the efficiency and mean measured effective radius. A low LWC cloud event would likely present  
647 a greater proportion of liquid water residing in smaller droplets; therefore, for a low LWC, we expected the  
648 collection efficiency to diminish owing to the cutoff diameter. However, this decrease was not observed in the  
649 cloud samples. Additional measurements of droplet size distribution during sampling would be beneficial for  
650 clarifying this issue.

651 We compared the collection efficiency and chemical compositions of the BOOGIE collector with two collectors  
652 that are commonly used by the scientific community to study cloud composition and environmental variability:  
653 the CWS and the CASCC2. For the four studied cloud events, the BOOGIE collector presented an elevated water

**a supprimé:** This new cloud water collector was compared with two other single-stage collectors that are commonly used by the scientific community to study cloud composition and environmental variability. We selected the CWS initially developed at the University of Vienna (Kruiz et al., 1993) and often deployed at mountainous sites such as Mount Sonnblick (Austria) and the PUY station. The impaction of the droplets occurs in a metallic plate horizontally installed in the collector, and it can be sampled under supercooled conditions. The other collector was one of the samplers developed by the California Institute of Technology (Caltech) for studies on fog and clouds (Daube et al., 1987), the CASCC2. This active sampler is a compact version of the CASCC, in which droplets are collected by impaction on a set of six rows of stainless-steel strings; it is highly efficient in terms of collection and is not affected by raindrops owing to its design by the using of a rain shield. It cannot function under supercooled conditions. The proposed BOOGIE collector aims to efficiently sample cloud droplets under warm cloud conditions and is designed to be easily sterilisable. Under low wind conditions, it is not affected by rain.

676 collection rate of  $82 \pm 32 \text{ mL h}^{-1}$  (CASCC2:  $62 \pm 30 \text{ mL h}^{-1}$ ; CWS:  $26 \pm 11 \text{ mL h}^{-1}$ ). This can be explained by the  
677 increased volume of cloudy air entering the new collector. On average, the calculated sampling efficiency was  $70$   
678  $\pm 10\%$  for BOOGIE, in the same range as that for CASCC2 and CWS. The chemical and biological compositions  
679 measured in the samples collected by the three collectors can be evaluated as comparable; however, some  
680 differences can be highlighted, which can be explained by the design of the collector, type of collection, and  
681 inhomogeneous chemical composition of the cloud condensation nuclei.

682 This BOOGIE collector is designed for use in field campaigns and long-term observatory sites. It contributes to  
683 the evaluation of the complex cloud water bio-physico-chemical composition, to the analysis of its environmental  
684 variability; it allows a sufficient volume of water to be collected to characterize the chemical and biological  
685 transformations occurring in it. This will help better constrain detailed cloud chemistry models that need to be  
686 validated (Barth et al., 2021). For future development, our team aims to reduce the size and weight of the collector  
687 such that it can be installed under a native balloon. The second development concerns the automation of this  
688 collector to initiate collection remotely and increase the sampling frequency. Finally, we aim to conduct intensive  
689 campaigns in the frame of the ACTRIS “Cloud In Situ” network to compare the collectors used by the scientific  
690 community at other measurement sites.

691 *Data availability:* All data are available through communication with the authors.

692 *Author contributions:* LD, MV were responsible of the project. MV, CBern and LD designed the new instrument,  
693 MR created the 3D plans of BOOGIE. CBert performed the CFD analysis. MV, AB and LD conducted the cloud  
694 sampling. MV and AB performed the chemical and biological analysis in the lab. [CG, CV and LD performed the](#)  
695 [physical measurements to estimate the air flow inside the collector.](#) LD and MV performed the data analysis. LD,  
696 MV and AB conducted scientific analyses. LD prepared the manuscript and designed the figures, with  
697 contributions from all authors.

698 *Competing interests.* The authors declare that they have no conflict of interest.

699 *Acknowledgments.* This study on cloud water characterisation was performed in the framework of the CO-PDD  
700 instrumented site of the OPGC observatory and LAMP laboratory. This study was supported by the Université  
701 Clermont Auvergne, Centre National de la Recherche Scientifique (CNRS), and Centre National d’Etudes  
702 Spatiales (CNES). The authors are also grateful for the support from the Fédération des Recherches en  
703 Environnement through the CPER funded by Region Auvergne–Rhône-Alpes, the French Ministry, ACTRIS  
704 Research Infrastructure, and FEDER European regional funds. The authors also thank I-Site CAP 20-25. We thank  
705 Olivier Masson from the IRSN for their CASCC2 collector, which was gratefully lent during the inter-comparison  
706 campaign.

707 *Financial support.* The authors are grateful to the Agence Nationale de la Recherche (ANR) for its financial  
708 support through the BIOCAP (ANR-13-BS06-0004) and METACLOUD (ANR-19-CE01-0004) projects. The first

709 project has financed the work of Mickaël Vaïtilingom during his post-doc at the LAMP laboratory and the second  
710 one allowed for their evaluation for specific scientific questions. We thank OPGC for additional funding and  
711 OPGC Service de développement technologique for manufacturing the cloud samplers. The Institut de Chimie de  
712 Clermont-Ferrand and Laboratoire Microorganismes: Génome Environnement laboratories are acknowledged for  
713 allowing access to their chemical and microbial analytical platforms.

#### 714 **References**

- 715 Adachi, K., Tobo, Y., Koike, M., Freitas, G., Zieger, P., and Krejci, R.: Composition and mixing state of Arctic  
716 aerosol and cloud residual particles from long-term single-particle observations at Zeppelin Observatory, Svalbard,  
717 *Atmos. Chem. Phys.*, 22, 14421-14439, 10.5194/acp-22-14421-2022, 2022.
- 718 Amato, P., Ménager, M., Sancelme, M., Laj, P., Mailhot, G., and Delort, A.-M.: Microbial population in cloud  
719 water at the puy de Dôme: Implications for the chemistry of clouds, *Atmos. Environ.*, 39, 4143-4153,  
720 <https://doi.org/10.1016/j.atmosenv.2005.04.002>, 2005.
- 721 Amato, P., Joly, M., Besaury, L., Oudart, A., Taib, N., Moné, A. I., Deguillaume, L., Delort, A.-M., and Debroas,  
722 D.: Active microorganisms thrive among extremely diverse communities in cloud water, *PLOS ONE*, 12,  
723 e0182869, 10.1371/journal.pone.0182869, 2017.
- 724 Baray, J. L., Deguillaume, L., Colomb, A., Sellegri, K., Freney, E., Rose, C., Van Baelen, J., Pichon, J. M., Picard,  
725 D., Fréville, P., Bouvier, L., Ribeiro, M., Amato, P., Banson, S., Bianco, A., Borbon, A., Bourcier, L., Bras, Y.,  
726 Brigante, M., Cacault, P., Chauvigné, A., Charbouillot, T., Chaumerliac, N., Delort, A. M., Delmotte, M., Dupuy,  
727 R., Farah, A., Febvre, G., Flossmann, A., Gourbeyre, C., Hervier, C., Hervo, M., Huret, N., Joly, M., Kazan, V.,  
728 Lopez, M., Mailhot, G., Marinoni, A., Masson, O., Montoux, N., Parazols, M., Peyrin, F., Pointin, Y., Ramonet,  
729 M., Rocco, M., Sancelme, M., Sauvage, S., Schmidt, M., Tison, E., Vaïtilingom, M., Villani, P., Wang, M., Yver-  
730 Kwok, C., and Laj, P.: Cézéaux-Aulnat-Opme-Puy De Dôme: a multi-site for the long-term survey of the  
731 tropospheric composition and climate change, *Atmos. Meas. Tech.*, 13, 3413-3445, 10.5194/amt-13-3413-2020,  
732 2020.
- 733 Barth, M. C., Ervens, B., Herrmann, H., Tilgner, A., McNeill, V. F., Tsui, W. G., Deguillaume, L., Chaumerliac,  
734 N., Carlton, A., and Lance, S. M.: Box model intercomparison of cloud chemistry, *J. Geophys. Res.: Atmos.*, 126,  
735 e2021JD035486, <https://doi.org/10.1029/2021JD035486>, 2021.
- 736 Bauer, H., Kasper-Giebl, A., Löflund, M., Giebl, H., Hitzenberger, R., Zibuschka, F., and Puxbaum, H.: The  
737 contribution of bacteria and fungal spores to the organic carbon content of cloud water, precipitation and aerosols,  
738 *Atmos. Res.*, 64, 109-119, [https://doi.org/10.1016/S0169-8095\(02\)00084-4](https://doi.org/10.1016/S0169-8095(02)00084-4), 2002.
- 739 Berner, A.: The collection of fog droplets by a jet impaction stage, *STOTEN*, 73, 217-228,  
740 [https://doi.org/10.1016/0048-9697\(88\)90430-5](https://doi.org/10.1016/0048-9697(88)90430-5), 1988.
- 741 Bianco, A., Deguillaume, L., Chaumerliac, N., Vaïtilingom, M., Wang, M., Delort, A.-M., and Bridoux, M. C.:  
742 Effect of endogenous microbiota on the molecular composition of cloud water: a study by Fourier-transform ion  
743 cyclotron resonance mass spectrometry (FT-ICR MS), *Sci. Rep.*, 9, 7663, 10.1038/s41598-019-44149-8, 2019.
- 744 Bianco, A., Deguillaume, L., Vaïtilingom, M., Nicol, E., Baray, J.-L., Chaumerliac, N., and Bridoux, M.:  
745 Molecular characterization of cloud water samples collected at the puy de Dôme (France) by Fourier Transform  
746 Ion Cyclotron Resonance Mass Spectrometry, *Environ. Sci. & Technol.*, 52, 10275-10285,  
747 10.1021/acs.est.8b01964, 2018.
- 748 Bianco, A., Vaïtilingom, M., Bridoux, M., Chaumerliac, N., Pichon, J.-M., Piro, J.-L., and Deguillaume, L.: Trace  
749 metals in cloud water sampled at the Puy de Dôme station, *Atmosphere*, 8, 225,  
750 <https://doi.org/10.3390/atmos8110225>, 2017.
- 751 Blando, J. D. and Turpin, B. J.: Secondary organic aerosol formation in cloud and fog droplets: a literature  
752 evaluation of plausibility, *Atmos. Environ.*, 34, 1623-1632, 10.1016/s1352-2310(99)00392-1, 2000.

753 Brantner, B., Fierlinger, H., Puxbaum, H., and Berner, A.: Cloudwater chemistry in the subcooled droplet regime  
754 at Mount Sonnblick (3106 M A.S.L., Salzburg, Austria), *Water, Air, and Soil Poll.*, 74, 363-384,  
755 10.1007/BF00479800, 1994.

756 Collett Jr, J. L., Daube Jr, B. C., Gunz, D., and Hoffmann, M. R.: Intensive studies of Sierra Nevada cloudwater  
757 chemistry and its relationship to precursor aerosol and gas concentrations, *Atmos. Environ.*, 24, 1741-1757,  
758 10.1016/0960-1686(90)90507-j, 1990.

759 Cook, R. D., Lin, Y. H., Peng, Z., Boone, E., Chu, R. K., Dukett, J. E., Gunsch, M. J., Zhang, W., Tolic, N., Laskin,  
760 A., and Pratt, K. A.: Biogenic, urban, and wildfire influences on the molecular composition of dissolved organic  
761 compounds in cloud water, *Atmos. Chem. Phys.*, 17, 15167-15180, 10.5194/acp-17-15167-2017, 2017.

762 Crosbie, E., Brown, M. D., Shook, M., Ziemba, L., Moore, R. H., Shingler, T., Winstead, E., Thornhill, K. L.,  
763 Robinson, C., MacDonald, A. B., Dadashazar, H., Sorooshian, A., Beyersdorf, A., Eugene, A., Collett Jr, J., Straub,  
764 D., and Anderson, B.: Development and characterization of a high-efficiency, aircraft-based axial cyclone cloud  
765 water collector, *Atmos. Meas. Tech.*, 11, 5025-5048, 10.5194/amt-11-5025-2018, 2018.

766 Daube, B., Kimball, K. D., Lamar, P. A., and Weathers, K. C.: Two new ground-level cloud water sampler designs  
767 which reduce rain contamination, *Atmos. Environ.*, 21, 893-900, [https://doi.org/10.1016/0004-6981\(87\)90085-0](https://doi.org/10.1016/0004-6981(87)90085-0),  
768 1987.

769 Deguillaume, L., Leriche, M., Amato, P., Ariya, P. A., Delort, A. M., Pöschl, U., Chaumerliac, N., Bauer, H.,  
770 Flossmann, A. I., and Morris, C. E.: Microbiology and atmospheric processes: chemical interactions of primary  
771 biological aerosols, *Biogeosciences*, 5, 1073-1084, 10.5194/bg-5-1073-2008, 2008.

772 Deguillaume, L., Charbouillot, T., Joly, M., Vaïtilingom, M., Parazols, M., Marinoni, A., Amato, P., Delort, A.  
773 M., Vinatier, V., Flossmann, A., Chaumerliac, N., Pichon, J. M., Houdier, S., Laj, P., Sellegri, K., Colomb, A.,  
774 Brigante, M., and Mailhot, G.: Classification of clouds sampled at the puy de Dôme (France) based on 10 yr of  
775 monitoring of their physicochemical properties, *Atmos. Chem. Phys.*, 14, 1485-1506, 10.5194/acp-14-1485-2014,  
776 2014.

777 Demoz, B. B., Collett, J. L., and Daube, B. C.: On the Caltech active strand cloudwater collectors, *Atmos. Res.*,  
778 41, 47-62, [https://doi.org/10.1016/0169-8095\(95\)00044-5](https://doi.org/10.1016/0169-8095(95)00044-5), 1996.

779 Dominutti, P. A., Renard, P., Vaïtilingom, M., Bianco, A., Baray, J. L., Borbon, A., Bourianne, T., Burnet, F.,  
780 Colomb, A., Delort, A. M., Duflot, V., Houdier, S., Jaffrezo, J. L., Joly, M., Leremboure, M., Metzger, J. M.,  
781 Pichon, J. M., Ribeiro, M., Rocco, M., Tulet, P., Vella, A., Leriche, M., and Deguillaume, L.: Insights into tropical  
782 cloud chemistry in Réunion (Indian Ocean): results from the BIO-MAÏDO campaign, *Atmos. Chem. Phys.*, 22,  
783 505-533, 10.5194/acp-22-505-2022, 2022.

784 Ehrenhauser, F. S., Khadapkar, K., Wang, Y., Hutchings, J. W., Delhomme, O., Kommalapati, R. R., Herckes, P.,  
785 Wornat, M. J., and Valsaraj, K. T.: Processing of atmospheric polycyclic aromatic hydrocarbons by fog in an urban  
786 environment, *Journal of Environmental Monitoring*, 14, 2566-2579, 10.1039/C2EM30336A, 2012.

787 Gioda, A., Mayol-Bracero, O. L., Scatena, F. N., Weathers, K. C., Mateus, V. L., and McDowell, W. H.: Chemical  
788 constituents in clouds and rainwater in the Puerto Rican rainforest: Potential sources and seasonal drivers, *Atmos.*  
789 *Environ.*, 68, 208-220, <https://doi.org/10.1016/j.atmosenv.2012.11.017>, 2013.

790 Gioda, A., Reyes-Rodríguez, G. J., Santos-Figueroa, G., Collett Jr, J. L., Decesari, S., Ramos, M. d. C. K. V.,  
791 Bezerra Netto, H. J. C., de Aquino Neto, F. R., and Mayol-Bracero, O. L.: Speciation of water-soluble inorganic,  
792 organic, and total nitrogen in a background marine environment: Cloud water, rainwater, and aerosol particles,  
793 *Journal of Geophys. Res.: Atmos.*, 116, <https://doi.org/10.1029/2010JD015010>, 2011.

794 Guo, J., Wang, Y., Shen, X., Wang, Z., Lee, T., Wang, X., Li, P., Sun, M., Collett Jr, J. L., Wang, W., and Wang,  
795 T.: Characterization of cloud water chemistry at Mount Tai, China: Seasonal variation, anthropogenic impact, and  
796 cloud processing, *Atmos. Environ.*, 60, 467-476, <http://dx.doi.org/10.1016/j.atmosenv.2012.07.016>, 2012.

797 Guyot, G., Gourbeyre, C., Febvre, G., Shcherbakov, V., Burnet, F., Dupont, J. C., Sellegri, K., and Jourdan, O.:  
798 Quantitative evaluation of seven optical sensors for cloud microphysical measurements at the Puy-de-Dôme  
799 Observatory, France, *Atmos. Meas. Tech.*, 8, 4347-4367, 10.5194/amt-8-4347-2015, 2015.

800 Herckes, P., Valsaraj, K. T., and Collett Jr, J. L.: A review of observations of organic matter in fogs and clouds:  
801 Origin, processing and fate, *Atmos. Res.*, 132-133, 434-449, 10.1016/j.atmosres.2013.06.005, 2013.

802 Herckes, P., Hannigan, M. P., Trenary, L., Lee, T., and Collett Jr, J. L.: Organic compounds in radiation fogs in  
803 Davis (California), *Atmos. Res.*, 64, 99-108, 10.1016/s0169-8095(02)00083-2, 2002.

804 Herrmann, H., Schaefer, T., Tilgner, A., Styler, S. A., Weller, C., Teich, M., and Otto, T.: Tropospheric aqueous-  
805 phase chemistry: Kinetics, mechanisms, and its coupling to a changing gas phase, *Chem. Rev.*, 115, 4259-4334,  
806 10.1021/cr500447k, 2015.

807 Hoffmann, M. R.: On the kinetics and mechanism of oxidation of aquated sulfur dioxide by ozone, *Atmos.*  
808 *Environ.*, 20, 1145-1154, 10.1016/0004-6981(86)90147-2, 1986.

809 Hu, W., Niu, H., Murata, K., Wu, Z., Hu, M., Kojima, T., and Zhang, D.: Bacteria in atmospheric waters: Detection,  
810 characteristics and implications, *Atmos. Environ.*, 179, 201-221, <https://doi.org/10.1016/j.atmosenv.2018.02.026>,  
811 2018.

812 Hutchings, J., Robinson, M., Mellwraith, H., Triplett Kingston, J., and Herckes, P.: The chemistry of intercepted  
813 clouds in Northern Arizona during the North American monsoon season, *Water, Air, and Soil Poll.*, 199, 191-202,  
814 10.1007/s11270-008-9871-0, 2009.

815 Joly, M., Amato, P., Deguillaume, L., Monier, M., Hoose, C., and Delort, A. M.: Quantification of ice nuclei active  
816 at near 0 °C temperatures in low-altitude clouds at the Puy de Dôme atmospheric station, *Atmos. Chem. Phys.*, 14,  
817 8185-8195, 10.5194/acp-14-8185-2014, 2014.

818 Kagawa, M., Katsuta, N., and Ishizaka, Y.: Chemical characteristics of cloud water and sulfate production under  
819 excess hydrogen peroxide in a high mountainous region of central Japan, *Water, Air, & Soil Pollution*, 232, 177,  
820 10.1007/s11270-021-05099-y, 2021.

821 Krusz, C., Berner, A., and Brandner, B.: A cloud water sampler for high wind speeds, *Proceedings of the*  
822 *EUROTRAC Symposium 1992* SPB Academic Publishing bv, 1993, 523-525,

823 Lamkaddam, H., Dommen, J., Ranjithkumar, A., Gordon, H., Wehrle, G., Krechmer, J., Majluf, F., Salionov, D.,  
824 Schmale, J., Bjelić, S., Carslaw, K. S., El Haddad, I., and Baltensperger, U.: Large contribution to secondary  
825 organic aerosol from isoprene cloud chemistry, *Science Advances*, 7, eabe2952, doi:10.1126/sciadv.abe2952,  
826 2021.

827 Laskin, A., Laskin, J., and Nizkorodov, S. A.: Chemistry of atmospheric brown carbon, *Chem. Rev.*, 115, 4335-  
828 4382, 10.1021/cr5006167, 2015.

829 Lawrence, C. E., Casson, P., Brandt, R., Schwab, J. J., Dukett, J. E., Snyder, P., Yerger, E., Kelting, D.,  
830 VandenBoer, T. C., and Lance, S.: Long-term monitoring of cloud water chemistry at Whiteface Mountain: the  
831 emergence of a new chemical regime, *Atmos. Chem. Phys.*, 23, 1619-1639, 10.5194/acp-23-1619-2023, 2023.

832 Lebedev, A. T., Polyakova, O. V., Mazur, D. M., Artaev, V. B., Canet, I., Lallement, A., Vařtilingom, M.,  
833 Deguillaume, L., and Delort, A. M.: Detection of semi-volatile compounds in cloud waters by GC×GC-TOF-MS.  
834 Evidence of phenols and phthalates as priority pollutants, *Environ. Poll.*, 241, 616-625,  
835 <https://doi.org/10.1016/j.envpol.2018.05.089>, 2018.

836 Li, J., Wang, X., Chen, J., Zhu, C., Li, W., Li, C., Liu, L., Xu, C., Wen, L., Xue, L., Wang, W., Ding, A., and  
837 Herrmann, H.: Chemical composition and droplet size distribution of cloud at the summit of Mount Tai, China,  
838 *Atmos. Chem. Phys.*, 17, 9885-9896, 10.5194/acp-17-9885-2017, 2017.

839 Li, P. H., Wang, Y., Li, Y.-H., Wang, Z. F., Zhang, H. Y., Xu, P. J., and Wang, W. X.: Characterization of  
840 polycyclic aromatic hydrocarbons deposition in PM<sub>2.5</sub> and cloud/fog water at Mount Taishan (China), *Atmos.*  
841 *Environ.*, 44, 1996-2003, 10.1016/j.atmosenv.2010.02.031, 2010.

842 Li, T., Wang, Z., Wang, Y., Wu, C., Liang, Y., Xia, M., Yu, C., Yun, H., Wang, W., Wang, Y., Guo, J., Herrmann,  
843 H., and Wang, T.: Chemical characteristics of cloud water and the impacts on aerosol properties at a subtropical  
844 mountain site in Hong Kong SAR, *Atmos. Chem. Phys.*, 20, 391-407, 10.5194/acp-20-391-2020, 2020.

845 Liu, Y., Lim, C. K., Shen, Z., Lee, P. K. H., and Nah, T.: Effects of pH and light exposure on the survival of  
846 bacteria and their ability to biodegrade organic compounds in clouds: implications for microbial activity in acidic  
847 cloud water, *Atmos. Chem. Phys.*, 23, 1731-1747, 10.5194/acp-23-1731-2023, 2023.

848 Löflund, M., Kasper-Giebl, A., Schuster, B., Giebl, H., Hitzemberger, R., and Puxbaum, H.: Formic, acetic, oxalic,  
849 malonic and succinic acid concentrations and their contribution to organic carbon in cloud water, *Atmos. Environ.*,  
850 36, 1553-1558, 10.1016/s1352-2310(01)00573-8, 2002.



851 Lüttke, J., Levsen, K., Acker, K., Wieprecht, W., and Möller, D.: Phenols and nitrated phenols in clouds at mount  
852 Brocken, *International Journal of Environ. Anal. Chem.*, 74, 69-89, 10.1080/03067319908031417, 1999.

853 MacDonald, A. B., Dadashazar, H., Chuang, P. Y., Crosbie, E., Wang, H., Wang, Z., Jonsson, H. H., Flagan, R.  
854 C., Seinfeld, J. H., and Sorooshian, A.: Characteristic vertical profiles of cloud water composition in marine  
855 stratocumulus clouds and relationships with precipitation, *Journal of Geophys. Res.: Atmos.*, 123, 3704-3723,  
856 <https://doi.org/10.1002/2017JD027900>, 2018.

857 Marinoni, A., Laj, P., Sellegri, K., and Mailhot, G.: Cloud chemistry at the puy de Dôme: variability and  
858 relationships with environmental factors, *Atmos. Chem. Phys.*, 4, 715-728, 10.5194/acp-4-715-2004, 2004.

859 Marinoni, A., Parazols, M., Brigante, M., Deguillaume, L., Amato, P., Delort, A.-M., Laj, P., and Mailhot, G.:  
860 Hydrogen peroxide in natural cloud water: Sources and photoreactivity, *Atmos. Res.*, 101, 256-263,  
861 10.1016/j.atmosres.2011.02.013, 2011.

862 Marple, V. A. and Willeke, K.: Impactor design, *Atmos. Environ.* (1967), 10, 891-896,  
863 [https://doi.org/10.1016/0004-6981\(76\)90144-X](https://doi.org/10.1016/0004-6981(76)90144-X), 1976.

864 Munger, J. W., Jacob, D. J., Waldman, J. M., and Hoffmann, M. R.: Fogwater chemistry in an urban atmosphere,  
865 *Journal of Geophys. Res.*, 88, 5109-5121, <https://doi.org/10.1029/JC088iC09p05109>, 1983.

866 Munger, J. W., Jacob, D. J., Daube, B. C., Horowitz, L. W., Keene, W. C., and Heikes, B. G.: Formaldehyde,  
867 glyoxal, and methylglyoxal in air and cloudwater at a rural mountain site in central Virginia, *Journal of Geophys.*  
868 *Res.*, 100, 9325-9333, 10.1029/95jd00508, 1995.

869 Pailler, L., Wirgot, N., Joly, M., Renard, P., Mouchel-Vallon, C., Bianco, A., Leriche, M., Sancelme, M., Job, A.,  
870 Patryl, L., Armand, P., Delort, A.-M., Chaumerliac, N., and Deguillaume, L.: Assessing the efficiency of water-  
871 soluble organic compound biodegradation in clouds under various environmental conditions, *Environ. Sci.:*  
872 *Atmos.*, 3, 731-748, 10.1039/D2EA00153E, 2023.

873 Pye, H. O. T., Nenes, A., Alexander, B., Ault, A. P., Barth, M. C., Clegg, S. L., Collett Jr, J. L., Fahey, K. M.,  
874 Hennigan, C. J., Herrmann, H., Kanakidou, M., Kelly, J. T., Ku, I. T., McNeill, V. F., Riemer, N., Schaefer, T.,  
875 Shi, G., Tilgner, A., Walker, J. T., Wang, T., Weber, R., Xing, J., Zaveri, R. A., and Zuend, A.: The acidity of  
876 atmospheric particles and clouds, *Atmos. Chem. Phys.*, 20, 4809-4888, 10.5194/acp-20-4809-2020, 2020.

877 Renard, P., Bianco, A., Baray, J.-L., Bridoux, M., Delort, A.-M., and Deguillaume, L.: Classification of clouds  
878 sampled at the puy de Dôme station (France) based on chemical measurements and air mass history matrices,  
879 *Atmosphere*, 11, 732, <https://doi.org/10.3390/atmos11070732>, 2020.

880 Renard, P., Brissy, M., Rossi, F., Leremboure, M., Jaber, S., Baray, J. L., Bianco, A., Delort, A. M., and  
881 Deguillaume, L.: Free amino acid quantification in cloud water at the Puy de Dôme station (France), *Atmos. Chem.*  
882 *Phys.*, 22, 2467-2486, 10.5194/acp-22-2467-2022, 2022.

883 Roman, P., Polkowska, Ż., and Namieśnik, J.: Sampling procedures in studies of cloud water composition: a  
884 review, *Critical Reviews in Environmental Science and Technology*, 43, 1517-1555,  
885 10.1080/10643389.2011.647794, 2013.

886 Rossi, F., Péguilhan, R., Turgeon, N., Veillette, M., Baray, J.-L., Deguillaume, L., Amato, P., and Duchaine, C.:  
887 Quantification of antibiotic resistance genes (ARGs) in clouds at a mountain site (puy de Dôme, central France),  
888 *STOTEN*, 865, 161264, <https://doi.org/10.1016/j.scitotenv.2022.161264>, 2023.

889 Schell, D., Georgii, H. W., Maser, R., Jaeschke, W., Arends, B. G., Kos, G. P. A., Winkler, P., Schneider, T.,  
890 Berner, A., and Kruisz, C.: Intercomparison of fog water samplers, *Tellus B*, 44, 612-631,  
891 <https://doi.org/10.1034/j.1600-0889.1992.t01-1-00014.x>, 1992.

892 Schurman, M. I., Boris, A., Desyaterik, Y., and Collett, J. J. L.: Aqueous secondary organic aerosol formation in  
893 ambient cloud water photo-oxidations, *AAQR*, 18, 15-25, 10.4209/aaqr.2017.01.0029, 2018.

894 Skarżyńska, K., Polkowska, Ż., and Namieśnik, J.: Sampling of atmospheric precipitation and deposits for analysis  
895 of atmospheric pollution, *Journal of Automated Methods and Management in Chemistry*, 2006, 026908,  
896 10.1155/JAMMC/2006/26908, 2006.

897 Sun, W., Fu, Y., Zhang, G., Yang, Y., Jiang, F., Lian, X., Jiang, B., Liao, Y., Bi, X., Chen, D., Chen, J., Wang, X.,  
898 Ou, J., Peng, P., and Sheng, G.: Measurement report: Molecular characteristics of cloud water in southern China

899 and insights into aqueous-phase processes from Fourier transform ion cyclotron resonance mass spectrometry,  
900 *Atmos. Chem. Phys.*, 21, 16631-16644, 10.5194/acp-21-16631-2021, 2021.

901 Sun, X., Wang, Y., Li, H., Yang, X., Sun, L., Wang, X., Wang, T., and Wang, W.: Organic acids in cloud water  
902 and rainwater at a mountain site in acid rain areas of South China, *Environmental Science and Pollution Research*,  
903 23, 9529-9539, 10.1007/s11356-016-6038-1, 2016.

904 Tenberken-Pötzsch, B., Schwikowski, M., and Gäggeler, H. W.: A method to sample and separate ice crystals and  
905 supercooled cloud droplets in mixed phased clouds for subsequent chemical analysis, *Atmos. Environ.*, 34, 3629-  
906 3633, [https://doi.org/10.1016/S1352-2310\(00\)00140-0](https://doi.org/10.1016/S1352-2310(00)00140-0), 2000.

907 Triesch, N., van Pinxteren, M., Engel, A., and Herrmann, H.: Concerted measurements of free amino acids at the  
908 Cape Verde Islands: High enrichments in submicron sea spray aerosol particles and cloud droplets, *Atmos. Chem.*  
909 *Phys.*, 21, 163-181, 10.5194/acp-21-163-2021, 2021.

910 Vaïtilingom, M., Deguillaume, L., Vinatier, V., Sancelme, M., Amato, P., Chaumerliac, N., and Delort, A.-M.:  
911 Potential impact of microbial activity on the oxidant capacity and organic carbon budget in clouds, *PNAS*, 110,  
912 559-564, 10.1073/pnas.1205743110, 2013.

913 Vaïtilingom, M., Attard, E., Gaiani, N., Sancelme, M., Deguillaume, L., Flossmann, A. I., Amato, P., and Delort,  
914 A.-M.: Long-term features of cloud microbiology at the puy de Dôme (France), *Atmos. Environ.*, 56, 88-100,  
915 10.1016/j.atmosenv.2012.03.072, 2012.

916 van Pinxteren, D., Neusüß, C., and Herrmann, H.: On the abundance and source contributions of dicarboxylic acids  
917 in size-resolved aerosol particles at continental sites in central Europe, *Atmos. Chem. Phys.*, 14, 3913-3928,  
918 10.5194/acp-14-3913-2014, 2014.

919 van Pinxteren, D., Fomba, K. W., Mertes, S., Müller, K., Spindler, G., Schneider, J., Lee, T., Collett, J. L., and  
920 Herrmann, H.: Cloud water composition during HCCT-2010: Scavenging efficiencies, solute concentrations, and  
921 droplet size dependence of inorganic ions and dissolved organic carbon, *Atmos. Chem. Phys.*, 16, 3185-3205,  
922 10.5194/acp-16-3185-2016, 2016.

923 van Pinxteren, D., Plewka, A., Hofmann, D., Müller, K., Kramberger, H., Svrčina, B., Bächmann, K., Jaeschke,  
924 W., Mertes, S., Collett Jr, J. L., and Herrmann, H.: Schmücke hill cap cloud and valley stations aerosol  
925 characterisation during FEBUKO (II): Organic compounds, *Atmos. Environ.*, 39, 4305-4320,  
926 10.1016/j.atmosenv.2005.02.014, 2005.

927 van Pinxteren, M., Fomba, K. W., Triesch, N., Stolle, C., Wurl, O., Bahlmann, E., Gong, X., Voigtländer, J., Wex,  
928 H., Robinson, T. B., Barthel, S., Zeppenfeld, S., Hoffmann, E. H., Roveretto, M., Li, C., Grosselin, B., Daële, V.,  
929 Senf, F., van Pinxteren, D., Manzi, M., Zabalegui, N., Frka, S., Gašparović, B., Pereira, R., Li, T., Wen, L., Li, J.,  
930 Zhu, C., Chen, H., Chen, J., Fiedler, B., von Tümpling, W., Read, K. A., Punjabi, S., Lewis, A. C., Hopkins, J. R.,  
931 Carpenter, L. J., Peeken, I., Rixen, T., Schulz-Bull, D., Monge, M. E., Mellouki, A., George, C., Stratmann, F.,  
932 and Herrmann, H.: Marine organic matter in the remote environment of the Cape Verde islands – an introduction  
933 and overview to the MarParCloud campaign, *Atmos. Chem. Phys.*, 20, 6921-6951, 10.5194/acp-20-6921-2020,  
934 2020.

935 Waldman, J. M., Munger, J. W., J., J. D., and Hoffmann, M. R.: Chemical characterization of stratus cloudwater  
936 and its role as a vector for pollutant deposition in a Los Angeles pine forest, *Tellus B*, 37B, 91-108,  
937 <https://doi.org/10.1111/j.1600-0889.1985.tb00058.x>, 1985.

938 Wang, M., Perroux, H., Fleuret, J., Bianco, A., Bouvier, L., Colomb, A., Borbon, A., and Deguillaume, L.:  
939 Anthropogenic and biogenic hydrophobic VOCs detected in clouds at the puy de Dôme station using Stir Bar  
940 Sorptive Extraction: Deviation from the Henry's law prediction, *Atmos. Res.*, 237, 104844,  
941 <https://doi.org/10.1016/j.atmosres.2020.104844>, 2020.

942 Wei, M., Xu, C., Chen, J., Zhu, C., Li, J., and Lv, G.: Characteristics of bacterial community in cloud water at Mt  
943 Tai: similarity and disparity under polluted and non-polluted cloud episodes, *Atmos. Chem. Phys.*, 17, 5253-5270,  
944 10.5194/acp-17-5253-2017, 2017.

945 Wieprecht, W., Acker, K., Mertes, S., Collett, J., Jaeschke, W., Brüggemann, E., Möller, D., and Herrmann, H.:  
946 Cloud physics and cloud water sampler comparison during FEBUKO, *Atmos. Environ.*, 39, 4267-4277,  
947 <https://doi.org/10.1016/j.atmosenv.2005.02.012>, 2005.

948 Wright, L. P., Zhang, L., Cheng, I., Aherne, J., and Wentworth, G. R.: Impacts and effects indicators of  
949 atmospheric deposition of major pollutants to various ecosystems - a review, *AAQR*, 18, 1953-1992,  
950 10.4209/aaqr.2018.03.0107, 2018.

951 Xu, C., Wei, M., Chen, J., Sui, X., Zhu, C., Li, J., Zheng, L., Sui, G., Li, W., Wang, W., Zhang, Q., and Mellouki,  
952 A.: Investigation of diverse bacteria in cloud water at Mt. Tai, China, *STOTEN*, 580, 258-265,  
953 <http://dx.doi.org/10.1016/j.scitotenv.2016.12.081>, 2017.

954 Zhao, Y., Hallar, A. G., and Mazzoleni, L. R.: Atmospheric organic matter in clouds: exact masses and molecular  
955 formula identification using ultrahigh-resolution FT-ICR mass spectrometry, *Atmos. Chem. Phys.*, 13, 12343-  
956 12362, 10.5194/acp-13-12343-2013, 2013.